AFB vs AW - impact on PDFs, SM parameters and BSM searches

J. Fiaschi, F. Giuli, F. Hautmann, S. Moretti

UNIVERSITY OF LIVERPOOL

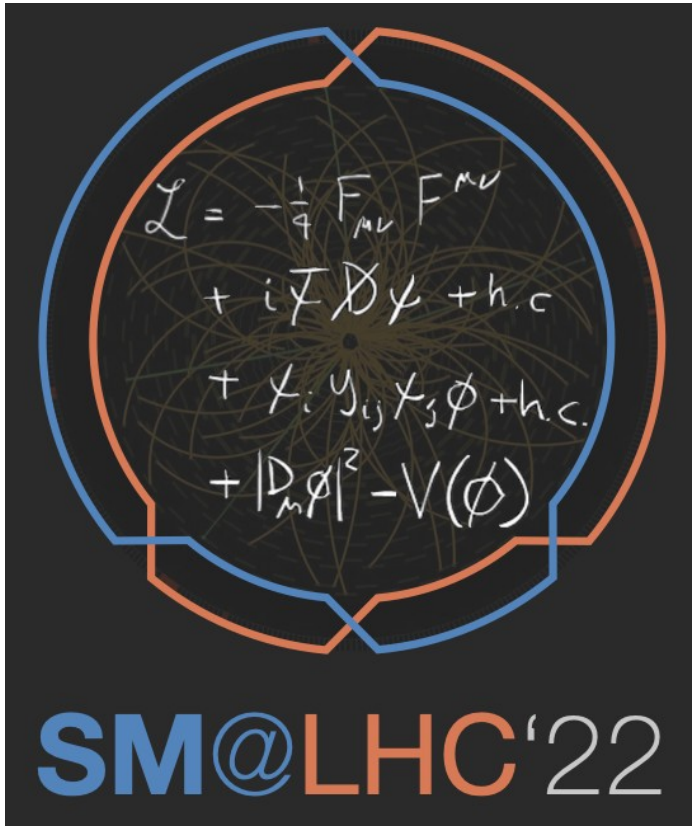

Topics of this talk

- **Drell-Yan data potential in PDF determination**

- **PDF profiling and impact on SM and BSM analyses:**
  - Including A_{FB} pseudodata
  - Combining A_W and A_{FB} pseudodata
  - Phenomenological studies

- **Conclusions**

Drell-Yan data

- **Drell-Yan data potential in PDF determination**

- **PDF profiling and impact on SM and BSM analyses:**
  - Including A_{FB} pseudodata
  - Combining A_W and A_{FB} pseudodata
  - Phenomenological studies

- **Conclusions**

The potential of Drell-Yan data

Drell-Yan measurements are capable of providing high sensitivity to PDFs as they feature low theoretical and experimental systematics, high statistical precision and good control of correlations.

We consider the impact of precision DY measurements on PDF determination and the consequences on BSM searches:

- the neutral channel **Forward-Backward Asymmetry (A_{FB})**
  (aka the angular coefficient A_4) JHEP 10 (2019) 176
- the charged channel **Lepton-charge Asymmetry (A_W)**
  Nucl.Phys.B 968 (2021) 115444
- the neutral channel angular coefficient A_0
  (relevant for Higgs physics, see backup slides) Phys.Lett.B 821 (2021) 136613

These quantities can be defined as ratio of cross sections:
- large cancellations of systematic uncertainties occour;
- good observables to include in PDF fits.

The potential of Drell-Yan data

Drell-Yan measurements are capable of providing high sensitivity to PDFs as they feature low theoretical and experimental systematics, high statistical precision and good control of correlations.

We consider the impact of precision DY measurements on PDF determination and the consequences on BSM searches:

- the neutral channel **Forward-Backward Asymmetry (A_{FB})** (aka the angular coefficient A_4) JHEP 10 (2019) 176
- the charged channel **Lepton-charge Asymmetry (A_W)** Nucl.Phys.B 968 (2021) 115444
- the neutral channel angular coefficient A_0 (relevant for Higgs physics, see backup slides) Phys.Lett.B 821 (2021) 136613

These quantities can be defined as ratio of cross sections:
- large cancellations of systematic uncertainties occour;
- good observables to include in PDF fits.

The xFitter framework

The **xFitter** code is an open-source QCD fit framework which:

- Allows for extraction of PDFs
- Assesses the impact of new measurements on PDF through Hessian profiling or Bayesian reweighting
- Evaluate consistency of experimental data
- Test various theoretical assumptions

Over 100 publications since the beginning of the project:
https://www.xfitter.org/xFitter/xFitter/results

Recent results:

Determination of Pion PDF: Phys. Rev. D 102, 014040 (2020)

Pion fragmentation functions (FF): Phys. Rev. D 104, 056019 (2021)

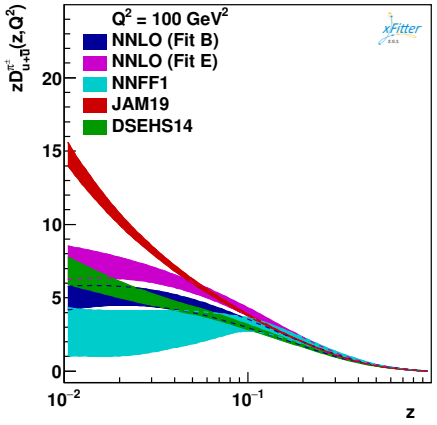

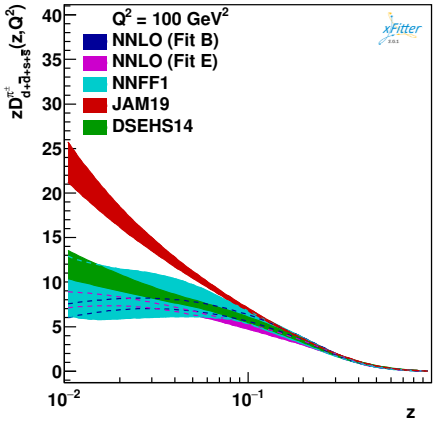

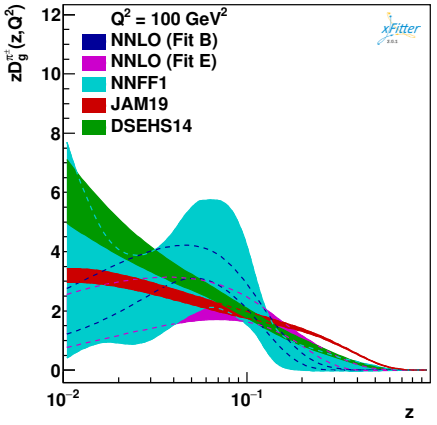

PDF profiling

- Drell-Yan data potential in PDF determination

- **PDF profiling and impact on SM and BSM analyses:**
  - Including A_{FB} pseudodata
  - Combining A_W and A_{FB} pseudodata
  - Phenomenological studies

- Conclusions

The Forward-Backward Asymmetry

$$A_{FB} = \frac{\sigma_F - \sigma_B}{\sigma_F + \sigma_B}$$

$$\sigma_F = \int_0^1 \frac{d\sigma}{d\cos\theta} d\cos\theta \quad , \quad \sigma_B = \int_{-1}^0 \frac{d\sigma}{d\cos\theta} d\cos\theta$$

Angle ***θ*** defined by the direction between the incoming quark and the lepton in the final state.

At the LHC we can observe the reconstructed A_{FB}*

At LO the direction of the incoming quark is defined by the boost of the di-lepton system.
At NLO the angle is defined in the Collins-Soper frame.

- Modern PDFs well describe existing experimental data.
- NLO corrections using MadGraph5_aMC@NLO interfaced to APPLgrid through aMCfast.
- **A_{FB}** pseudodata for 13 TeV LHC with precision corresponding to integrated luminosities stages of **30 fb^{-1} , 300 fb^{-1} and 3000 fb^{-1}**, including detector acceptance and efficiency in the di-electron final state.
- Different lower rapidity cuts considered

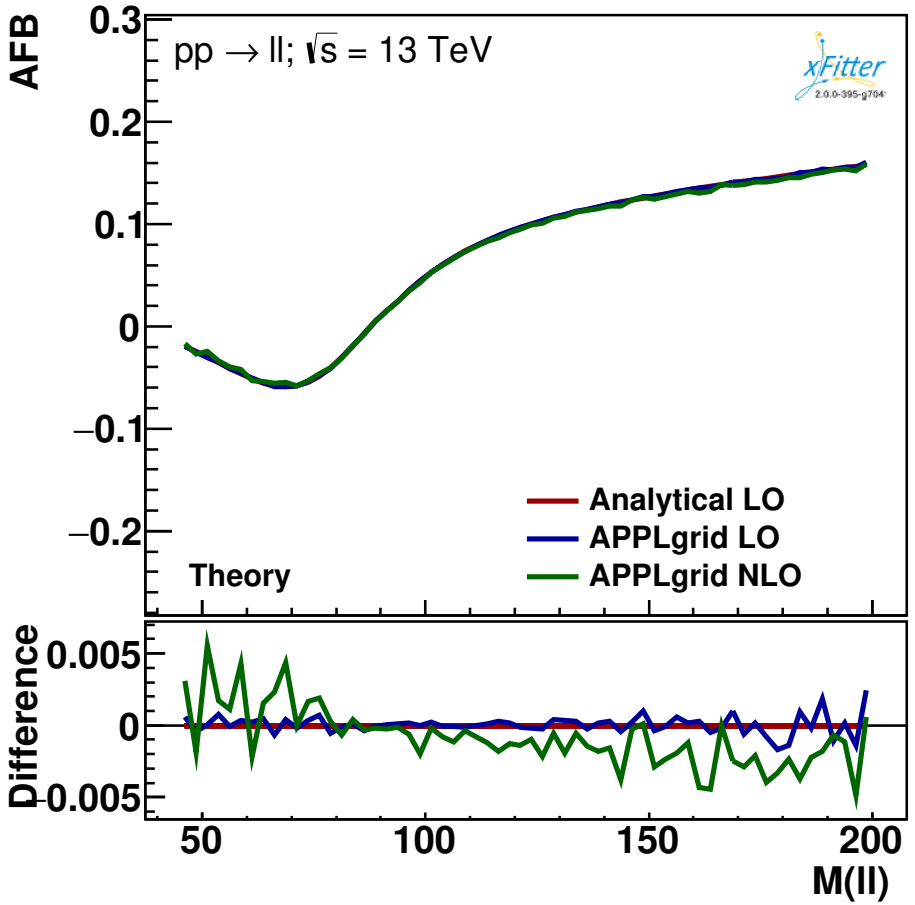

Profiling with A_{FB}

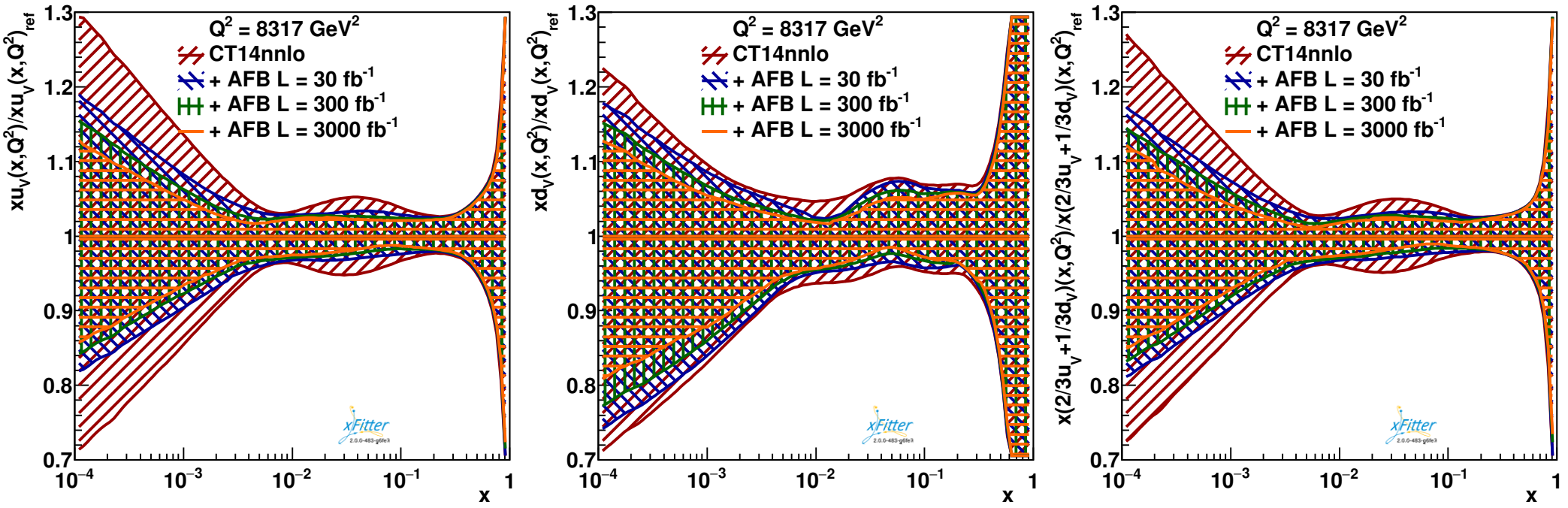

- **A_{FB}** (related to the angular coefficient $A_4 = 8/3\ A_{FB}$) is parity violating and sensitive to the flavor non-singlet PDFs.
- Sensitive to **$\sin^2\theta_w$** however the results of the analysis are rubust against variations in the choice of this parameter.
- The profiling with A_{FB} pseudodata leads to large reductions of uncertanty on *u* and *d* valence quarks PDFs, and particularly on the linear combination **$2/3u_v + 1/3d_v$** .
- Improvement is concentrated in low and intermediate Bjorken *x* regions.

Profiling with A_{FB}

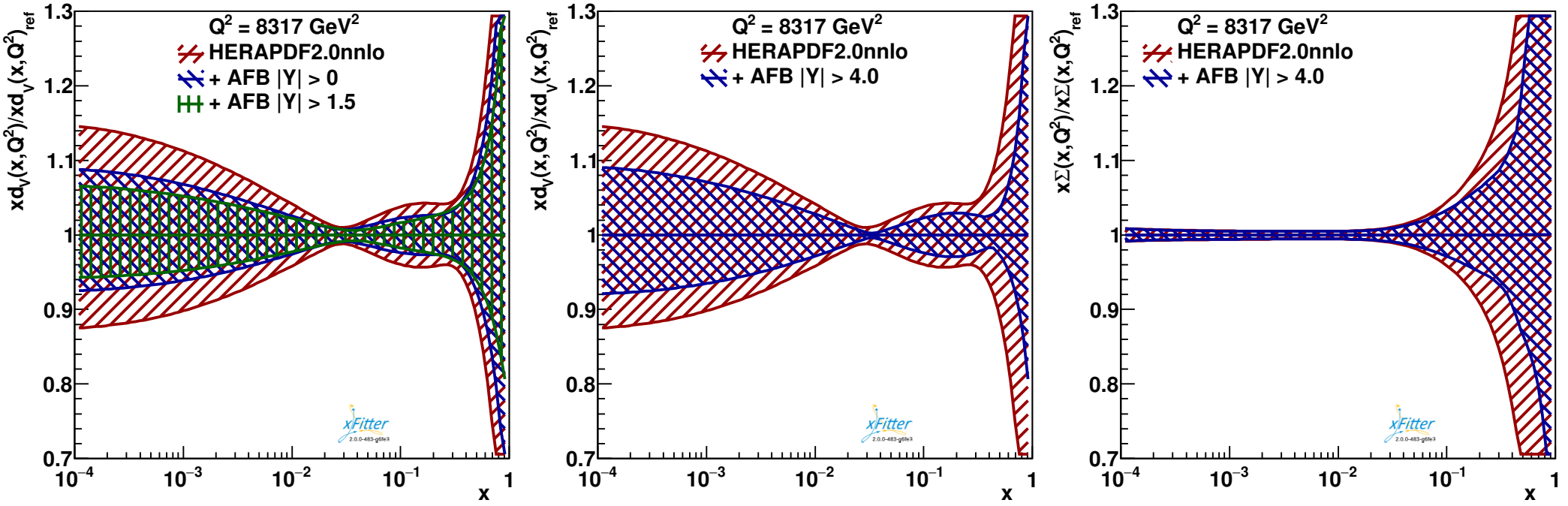

L = 3000 fb^{-1}

- High-*x* regions can be accessed applying specific rapidity cuts.
- Remarkable improvement in valence and sea quark distributions for $x > 10^{-1}$ when employing A_{FB} pseudodata in the very high rapidity region.
- The reduced statistic due to the strong rapidity cuts requires high integrated luminosity.

The Lepton-charge asymmetry

$$A_W = \frac{d\sigma_{W+}/d\eta_\ell - d\sigma_{W-}/d\eta_\ell}{d\sigma_{W+}/d\eta_\ell + d\sigma_{W-}/d\eta_\ell}$$

Calculations at **NLO QCD** accuracy, supplemented with **NNLO QCD** correction through **K-factor**.

Modern PDF sets well describe A_W data

PDF set	χ^2/d.o.f.
CT18NNLO	10.26/11
CT18ANNLO	11.29/11
MSHT20nnlo_as118	12.18/11
NNPDF3.1_nnlo_as_0118_hessian	14.88/11
PDF4LHC15_nnlo_100	9.53/11
ABMP16_5_nnlo	18.21/11
HERAPDF20_NNLO_EIG	8.92/11

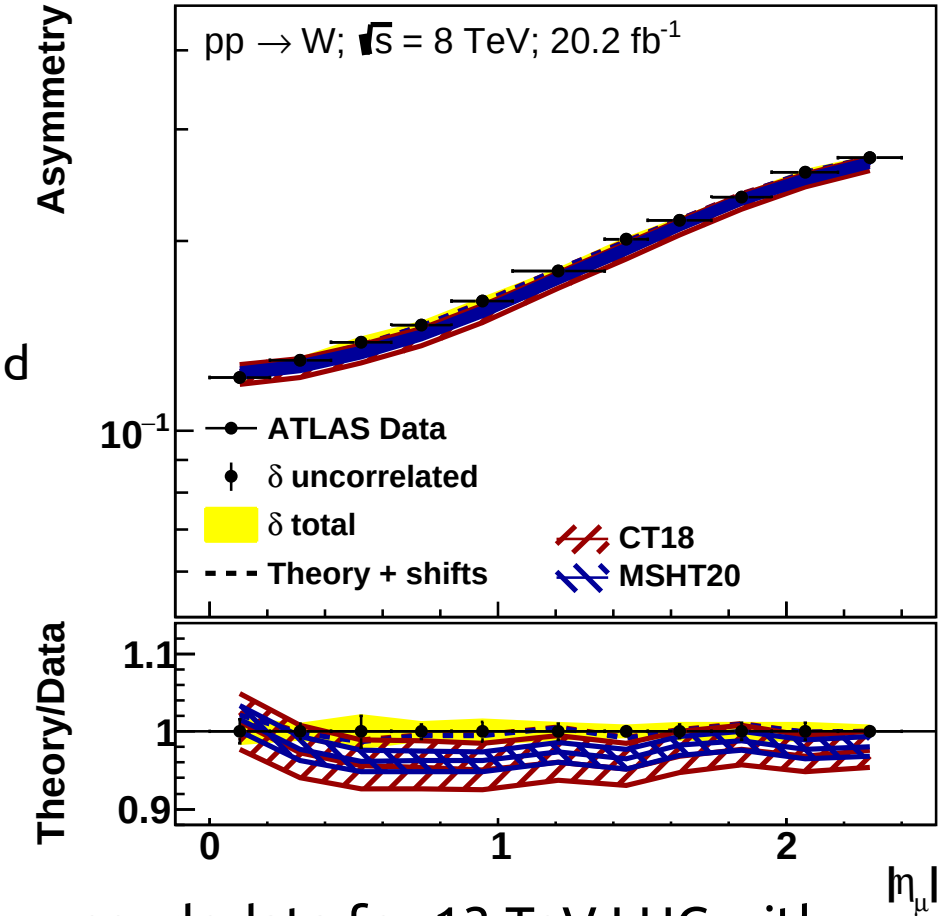

A_W pseudodata for 13 TeV LHC with precision corresponding to integrated luminosities stages:

- 300 fb^{-1} (end of LHC Run-III)
- 3000 fb^{-1} (HL-LHC stage)

Combining A_W and A_{FB}

CT18NNLO + A_{FB} + A_W

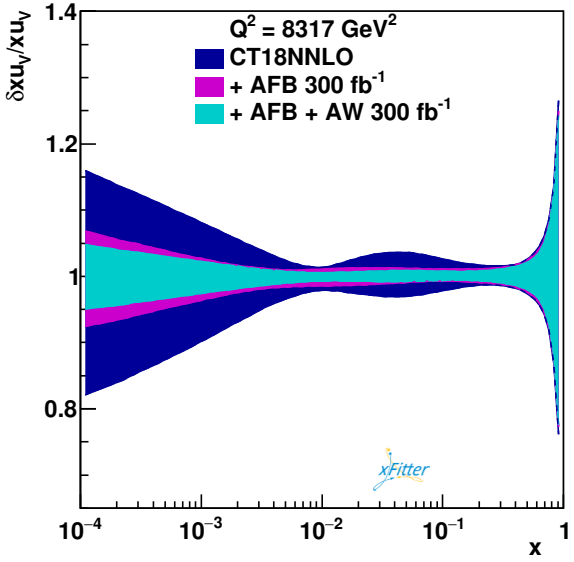

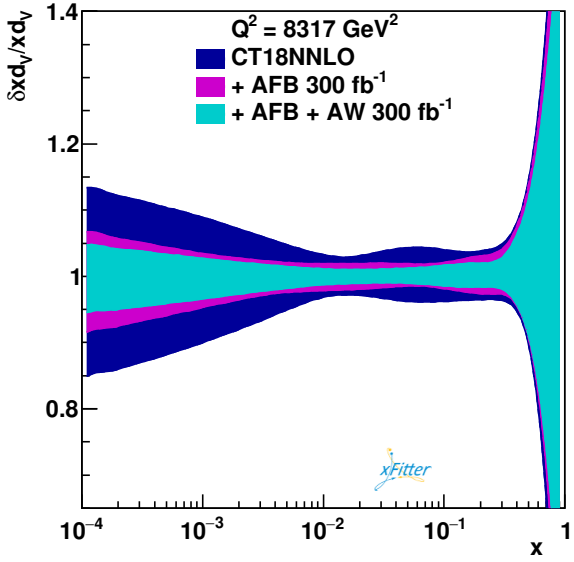

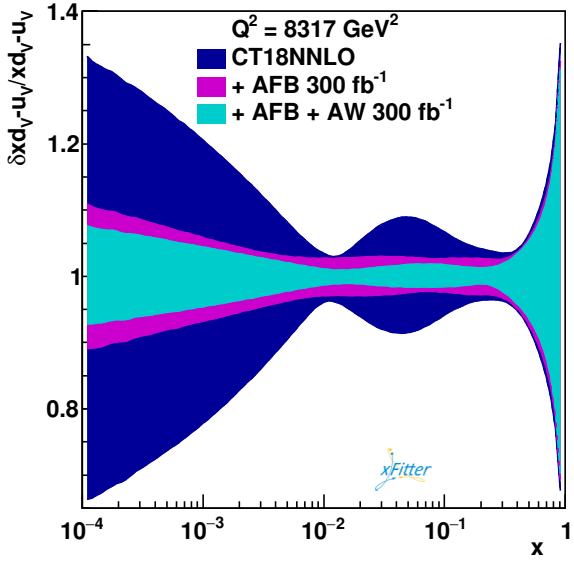

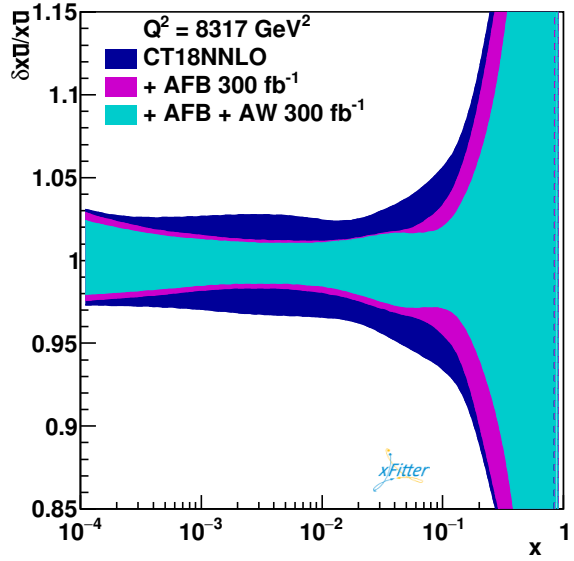

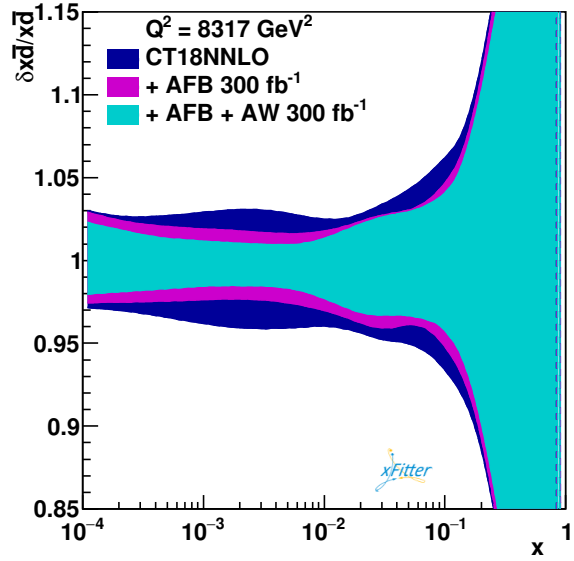

Saturation of uncertainty reduction from 300 fb^{-1} to 3000 fb^{-1}.

- Visible reduction in valence quark PDFs in low and intermediate x region.
- $\mathbf{A_W}$ most sensitive to the combination $\mathbf{d_V - u_V}$.
- The combination of $\mathbf{A_W}$ and $\mathbf{A_{FB}}$ can further reduce the PDF error bands.
- Large reduction in $\bar{u}$ PDF in the high *x* region and in $\bar{d}$ PDF in the intermediate *x* region.

A_W for proton antimatter asymmetry

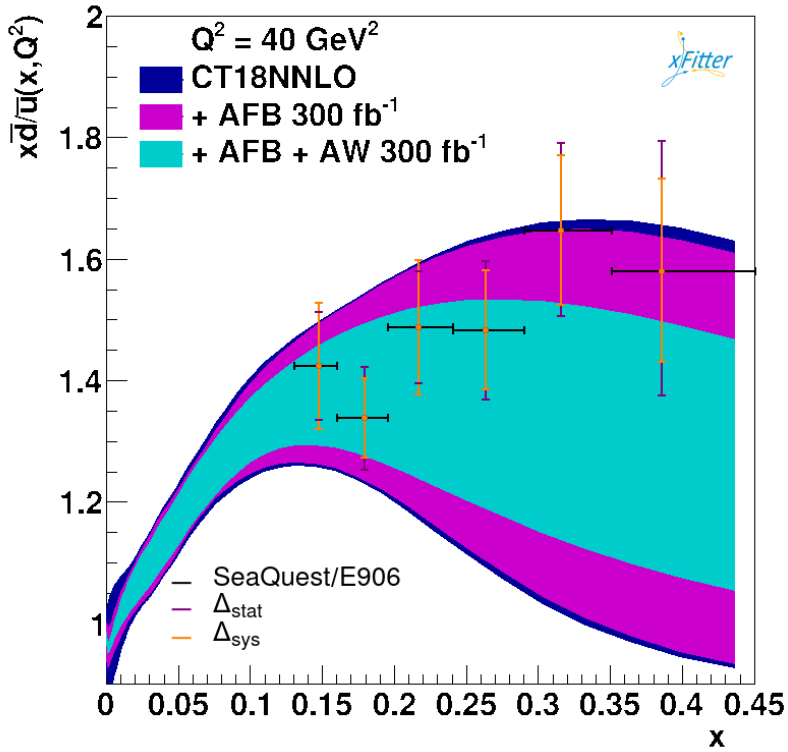

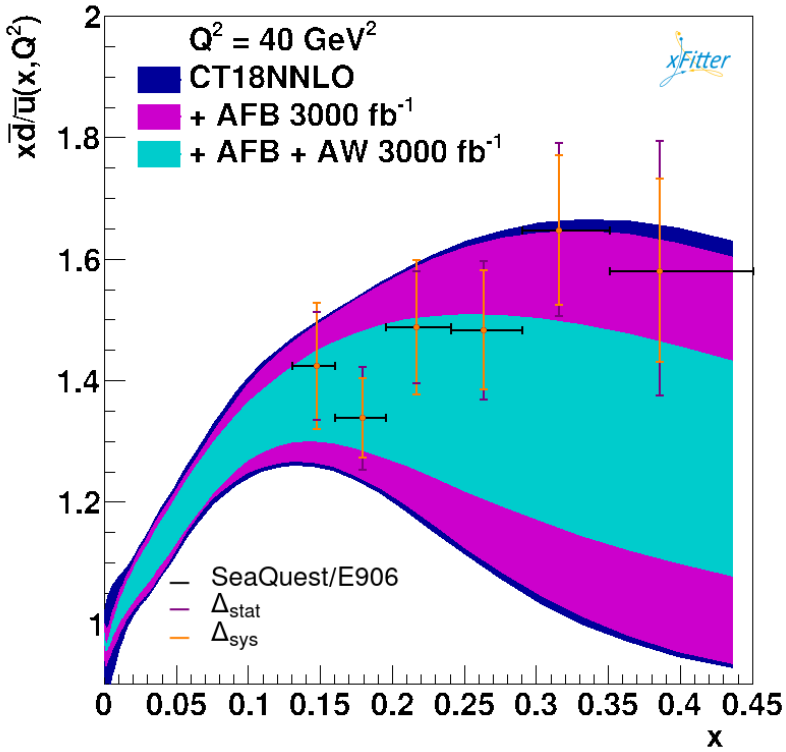

SeaQuest Collaboration,
Nature 590 (2021) 7847, 561-565

A_W data carries relevant information on the anti-quark PDFs in the high x region, and would provide a significant reduction of uncertainty bands in the region of interest.

(REMARK: real data would most certainly modify the central values as well)

BSM high mass searches

Significant reduction of uncertainties in the high transverse/invariant mass spectra for BSM searches.

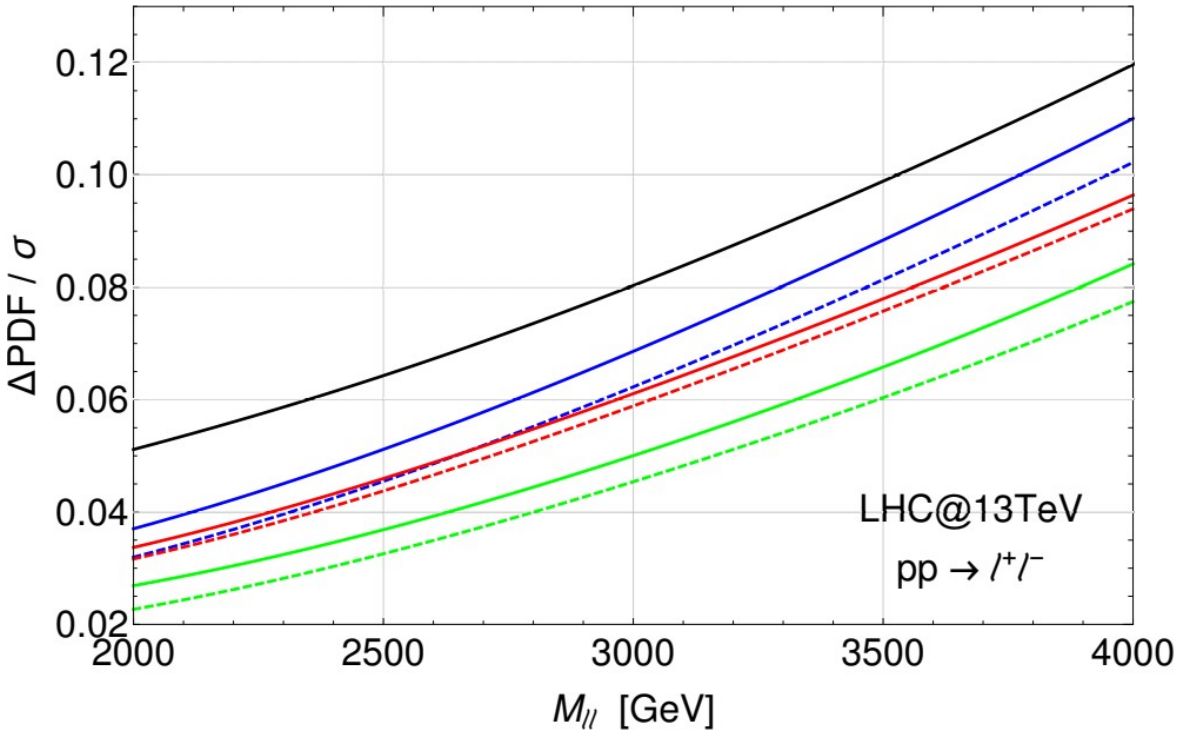

Dilepton high invariant mass:

- CT18NNLO
- CT18NNLO + A_{FB} 300 fb^{-1}
- CT18NNLO + A_{FB} 3000 fb^{-1}
- CT18NNLO + A_W 300 fb^{-1}
- CT18NNLO + A_W 3000 fb^{-1}
- CT18NNLO + A_{FB} + A_W 300 fb^{-1}
- CT18NNLO + A_{FB} + A_W 3000 fb^{-1}

Original PDF uncertainty (i.e.) at 4 TeV from 12% is reduced to:

- 11% (10.2%) by $\mathbf{A_{FB}}$ 300 (3000) fb^{-1} data
- 9.6% (9.4%) by $\mathbf{A_W}$ 300 (3000) fb^{-1} data
- 8.4% (7.8%) by combination of $\mathbf{A_{FB}}$ and $\mathbf{A_W}$ 300 (3000) fb^{-1} data

BSM resonances detection

PDF uncertainties are relevant in searches for non-resonant objects.

Benchmark: Enhanced SSM model
(same as SSM with BSM gauge coupling augmented by factor 3)

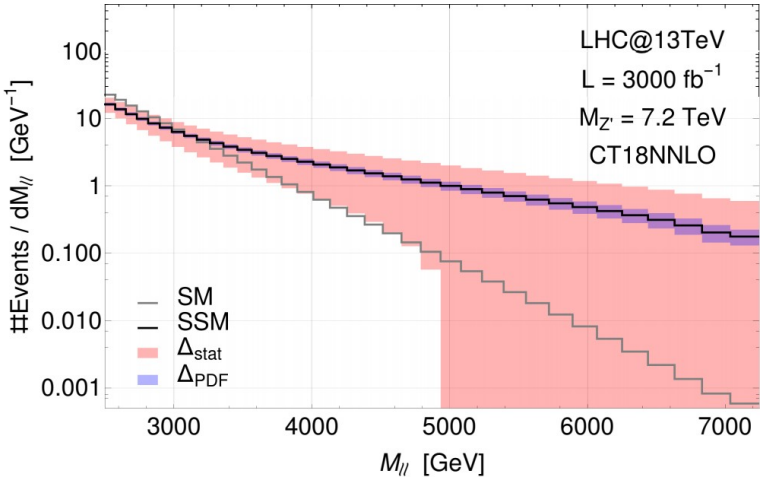

High invariant mass excess is non-significant

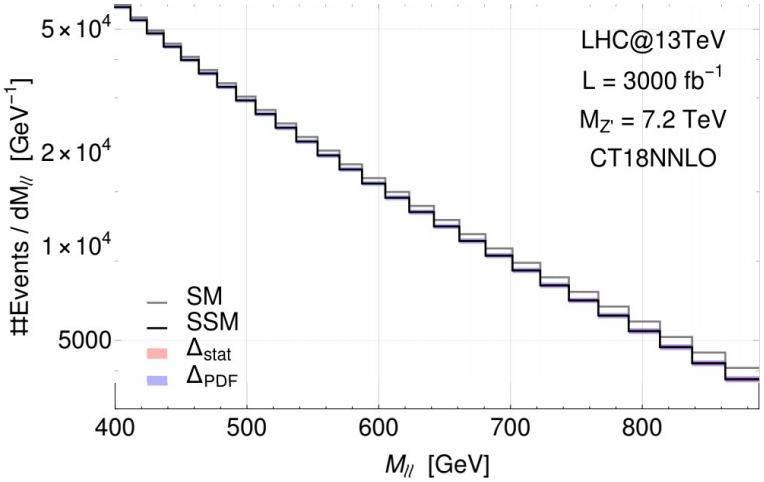

Significant depletion of events due to interference in the low invariant mass tail

Phys.Lett.B 803 (2020) 135293

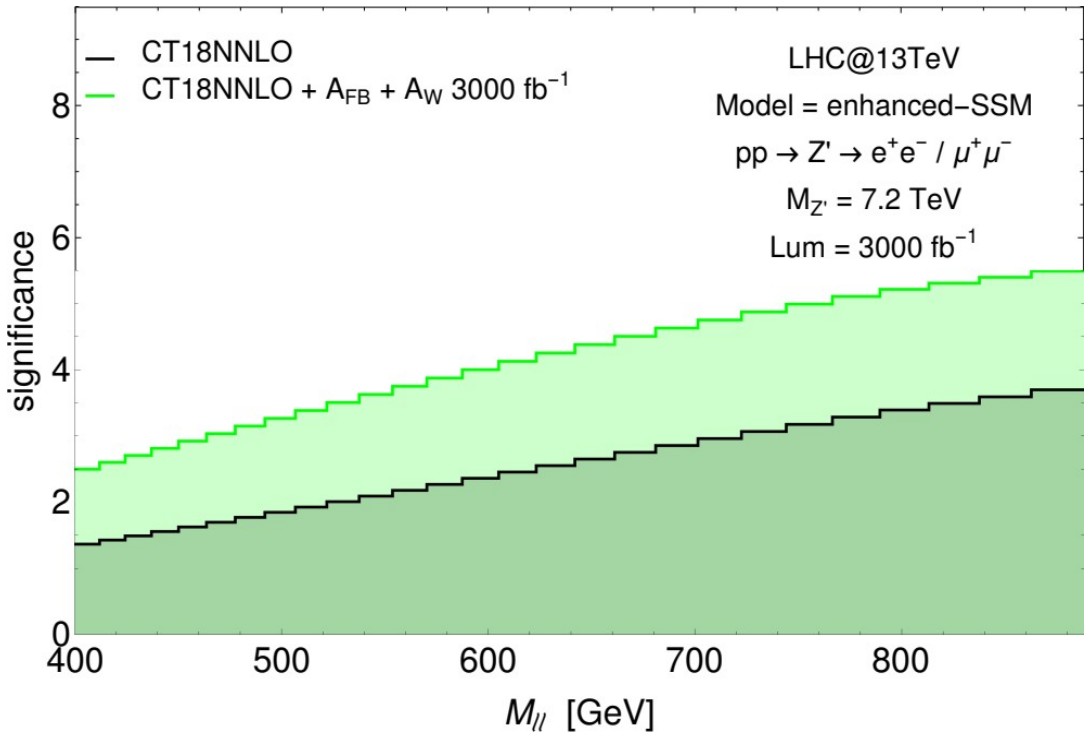

Early evidence of BSM physics significantly improved by reduction of PDF uncertainty

Case study: the 4DCHM

- **The Higgs boson is a bound state arising from a strong dynamics.**
  - The Higgs boson is a pseudo Naumbu-Goldstone boson from the breaking G → H
  - The most studied in the literature is the case of *SO(5) / SO(4)*

Agashe, Contino, Pomarol,
Nucl. Phys. B719, (2005), 183

- **The particle content of the model is:**
  - **5 Z'** (only Z_2, Z_3 and Z_5 coupled to the SM)
  - **3 W'** (only W_2 and W_3 coupled to the SM)

The BSM gauge bosons can have arbitrary width depending on the opened decay channels (particularly the ones associated to their decay into exotic heavy fermions).

- **Relevant model parameters:**
  - New gauge coupling g_ρ
  - Compositness scale f

- **Gauge boson masses:**
  - For Z_2, Z_3 and W_2 roughly $m_\rho = f\, g_\rho$
  - For Z_5 and W_3 roughly $\sqrt{2} m_\rho$
  - Fine corrections proportional to $\xi = v^2 / f^2$ after the symmetries breaking.

BSM searches in the 4DCHM

Peak region

Dip region

Neutral channel

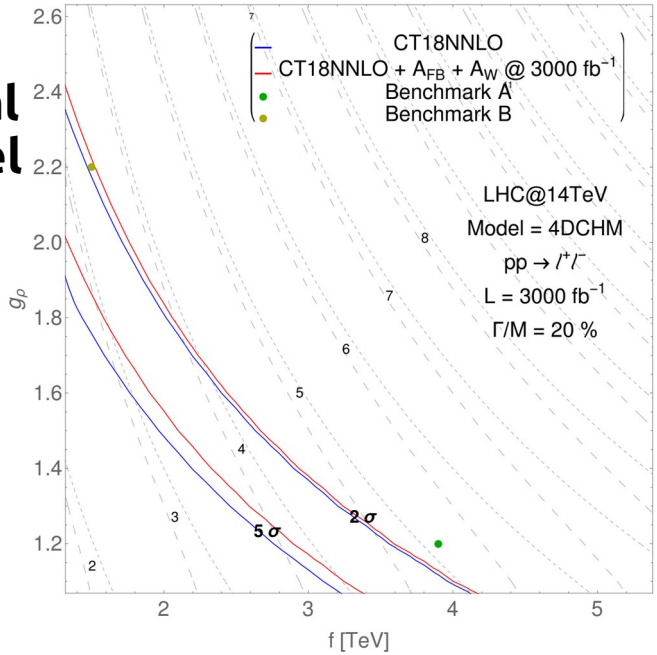

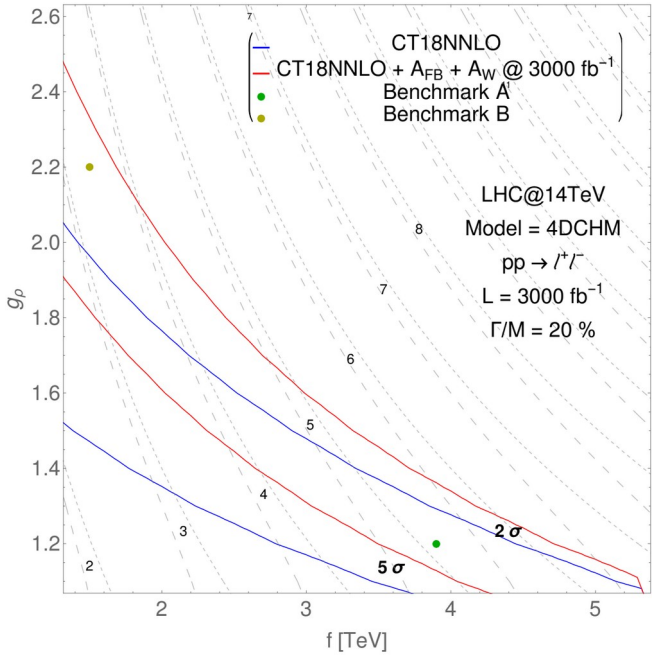

Charged channel

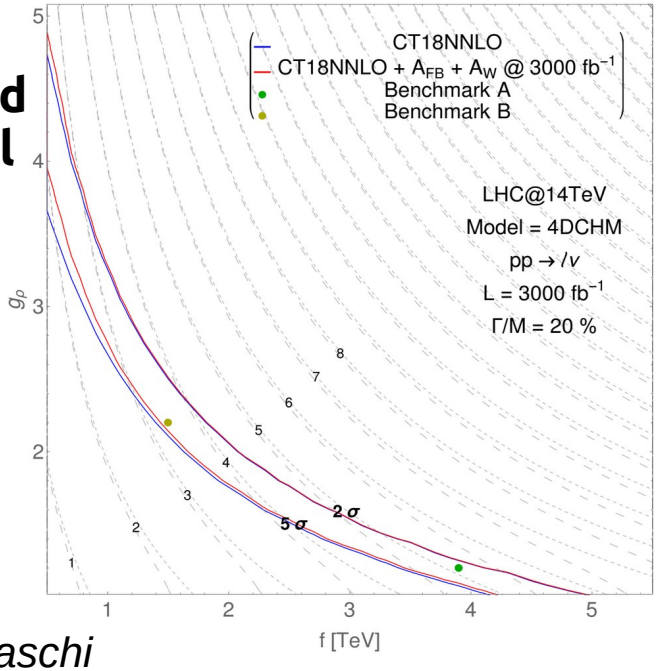

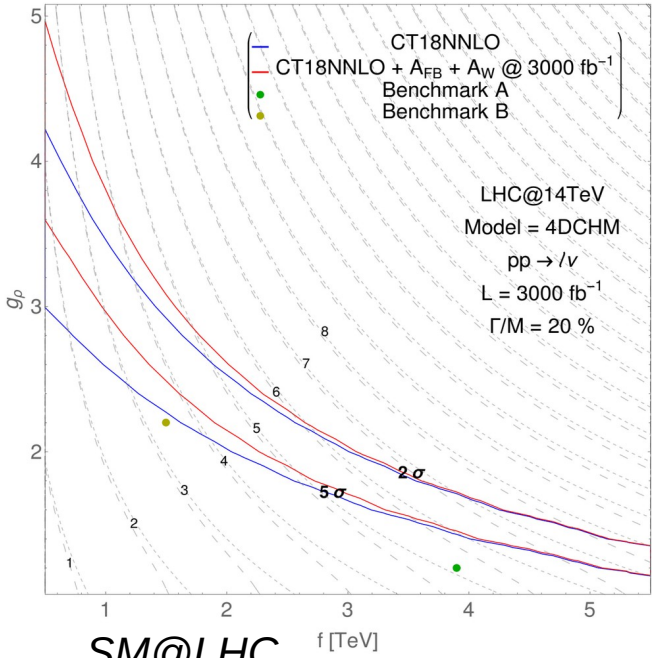

- Depletion of events in the dip region from strong interference effects in the neutral channel can be used to set strong model dependent constrains.
- Predictions for the dip region are sensibly improved by the profiling.
- Searches in the charged channel are more constraining.
- In the charged channel smaller improvement from PDF profiling in the dip region because of milder interference effects.
- Combined searches can improve the limits exploiting the correlation between neutral and charged resonances.

BSM searches in the 4DCHM

Benchmark resonances sensitivities: Neutral channel

Peak

Benchmark A			
inf [TeV]	sup [TeV]	σ_{SM} [fb]	σ_{SM+BSM} [fb]
4.99	8.90	$1.36 \cdot 10^{-4}$	$3.87 \cdot 10^{-4}$
Δ_{PDF} base [fb]	Δ_{PDF} profiled [fb]	α (base)	α (profiled)
$8.1 \cdot 10^{-5}$	$5.6 \cdot 10^{-5}$	1.31	1.35
Benchmark B			
inf [TeV]	sup [TeV]	σ_{SM} [fb]	σ_{SM+BSM} [fb]
3.36	5.52	$5.97 \cdot 10^{-3}$	$8.34 \cdot 10^{-3}$
Δ_{PDF} base [fb]	Δ_{PDF} profiled [fb]	α (base)	α (profiled)
$9.9 \cdot 10^{-4}$	$5.8 \cdot 10^{-4}$	1.88	2.10

Dip

Benchmark A			
inf [TeV]	sup [TeV]	σ_{SM} [fb]	σ_{SM+BSM} [fb]
2.06	4.99	$1.69 \cdot 10^{-1}$	$1.42 \cdot 10^{-1}$
Δ_{PDF} base [fb]	Δ_{PDF} profiled [fb]	α (base)	α (profiled)
$9.5 \cdot 10^{-3}$	$4.6 \cdot 10^{-3}$	3.34	4.82
Benchmark B			
inf [TeV]	sup [TeV]	σ_{SM} [fb]	σ_{SM+BSM} [fb]
1.36	3.36	1.53	1.45
Δ_{PDF} base [fb]	Δ_{PDF} profiled [fb]	α (base)	α (profiled)
$6.8 \cdot 10^{-2}$	$3.1 \cdot 10^{-2}$	1.53	2.91

Benchmark A

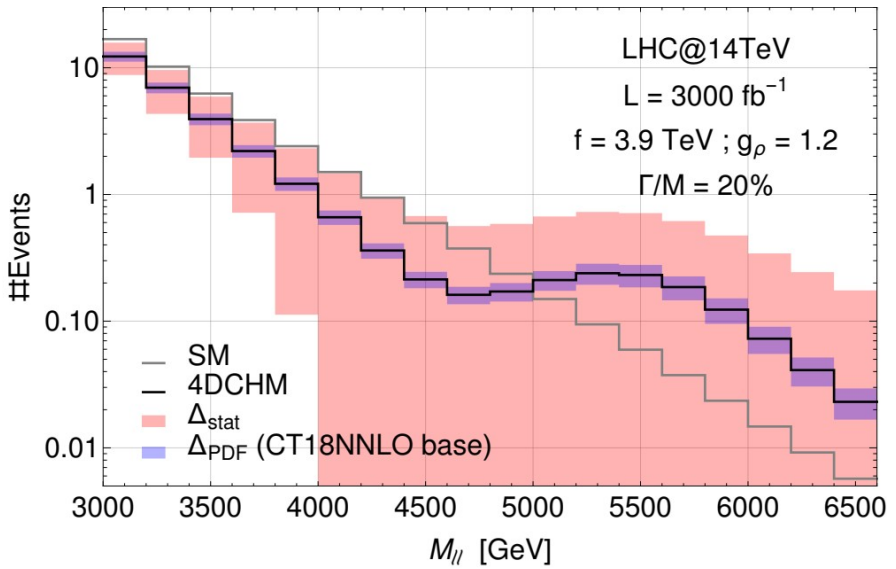

Benchmark B

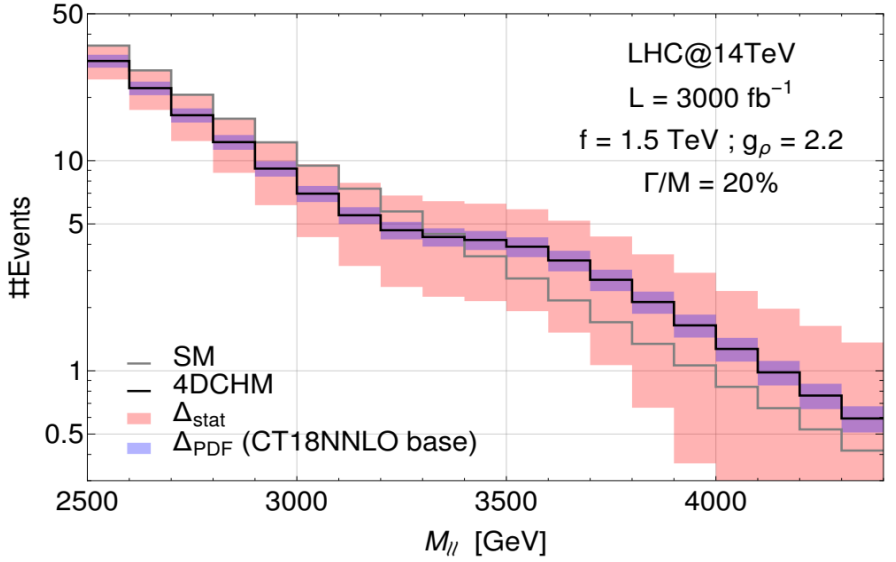

BSM searches in the 4DCHM

Benchmark resonances sensitivities: Charged channel

Peak

Benchmark A			
inf [TeV]	sup [TeV]	σ_{SM} [fb]	σ_{SM+BSM} [fb]
4.11	8.90	$8.13 \cdot 10^{-4}$	$3.51 \cdot 10^{-3}$
Δ_{PDF} base [fb]	Δ_{PDF} profiled [fb]	α (base)	α (profiled)
$6.1 \cdot 10^{-4}$	$5.3 \cdot 10^{-4}$	2.69	2.75
Benchmark B			
inf [TeV]	sup [TeV]	σ_{SM} [fb]	σ_{SM+BSM} [fb]
3.03	5.52	$1.22 \cdot 10^{-2}$	$2.36 \cdot 10^{-2}$
Δ_{PDF} base [fb]	Δ_{PDF} profiled [fb]	α (base)	α (profiled)
$2.3 \cdot 10^{-3}$	$1.9 \cdot 10^{-3}$	4.00	4.24

Dip

Benchmark A			
inf [TeV]	sup [TeV]	σ_{SM} [fb]	σ_{SM+BSM} [fb]
2.22	4.11	$1.07 \cdot 10^{-1}$	$5.71 \cdot 10^{-2}$
Δ_{PDF} base [fb]	Δ_{PDF} profiled [fb]	α (base)	α (profiled)
$3.7 \cdot 10^{-3}$	$2.7 \cdot 10^{-3}$	11.16	12.21
Benchmark B			
inf [TeV]	sup [TeV]	σ_{SM} [fb]	σ_{SM+BSM} [fb]
1.38	3.03	1.60	1.36
Δ_{PDF} base [fb]	Δ_{PDF} profiled [fb]	α (base)	α (profiled)
$5.7 \cdot 10^{-2}$	$3.6 \cdot 10^{-2}$	5.51	7.89

Benchmark A

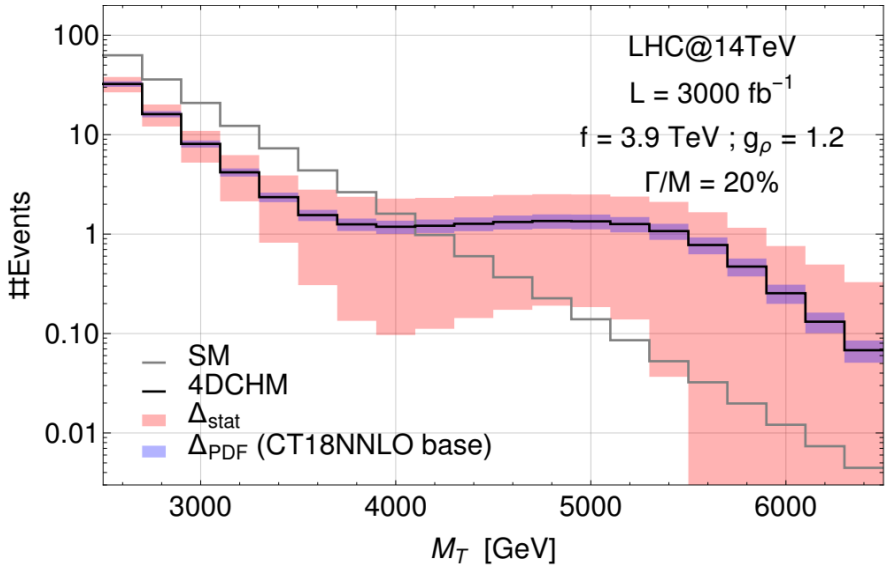

Benchmark B

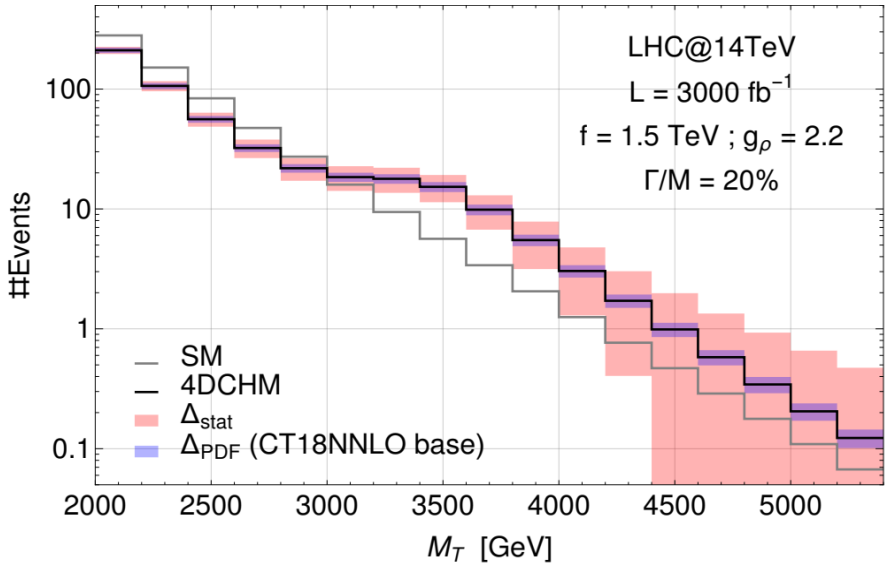

Conclusions

- **Drell-Yan data potential in PDF determination**

- **PDF profiling and impact on SM and BSM analyses:**
  - Including A_{FB} pseudodata
  - Combining A_W and A_{FB} pseudodata
  - Phenomenological studies

- **Conclusions**

Conclusions

- PDF uncertainties represent a strong limiting factor in the estraction of many SM quantities as well as in the sensitivity to certain BSM searches.

- Drell-Yan data has the potential to set important constraints on PDF determination, thanks to its experimental high statistical precision and high accuracy of the theoretical predictions.

- We assessed the impact of future DY neutral ($\mathbf{A_{FB}}$) and charged ($\mathbf{A_W}$) asymmetries data on PDF determination through a profiling:
  - Strong constraints on valence quark PDFs, comparable sensitivity of A_W and A_{FB}.
  - Significant constraints on anti-quark PDFs, particularly from A_W measurements at high *x*.

- Reduction of PDF uncertainties will consequently improve:
  - the determination of SM quantites.
  - the sensitivity in BSM searches (particularly for non-resonant states).

- Future prospects:
  - Simultaneous fit to all the angular coefficients $\mathbf{A_i}$ ($\mathbf{A_0}$ already studied, see backup)
  - Dedicated analysis on M_W and $sin^2\theta_W$ determination.

Thank you!

Backup slides

Neutral Drell-Yan

Expansion of the full differential cross section in therms of the angular coefficients $\mathbf{A_i}$:

$$\frac{\mathrm{d}\sigma}{\mathrm{d}p_{\mathrm{T}}^{Z}\,\mathrm{d}y^{Z}\,\mathrm{d}m^{Z}\,\mathrm{d}\cos\theta\,\mathrm{d}\phi} = \frac{3}{16\pi}\frac{\mathrm{d}\sigma^{U+L}}{\mathrm{d}p_{\mathrm{T}}^{Z}\,\mathrm{d}y^{Z}\,\mathrm{d}m^{Z}}$$

Unpolarised cross-section

$$\Big\{(1+\cos^2\theta) + \frac{1}{2}A_0(1-3\cos^2\theta) + A_1\,\sin 2\theta\,\cos\phi$$

Helicity cross-sections

$$+\frac{1}{2}A_2\,\sin^2\theta\,\cos 2\phi + A_3\,\sin\theta\,\cos\phi + A_4\,\cos\theta$$

$$+A_5\,\sin^2\theta\,\sin 2\phi + A_6\,\sin 2\theta\,\sin\phi + A_7\,\sin\theta\,\sin\phi\Big\}.$$

Phys.Lett.B 821 (2021) 136613

JHEP 10 (2019) 176

Angles measured in the Collins-Soper frame

Drell-Yan angular coefficients

$$< 1 + \cos^2\theta >$$

Normalization of the unpolarised cross-section

$$< \frac{1}{2}(1 - 3\cos^2\theta) >= \frac{3}{20}(A_0 - \frac{2}{3})$$

Longitudinal polarisation

$$< \sin 2\theta \ \cos\phi >= \frac{1}{5}A_1$$

Interference term: longitudinal/transverse

$$< \sin^2\theta \ \cos 2\phi >= \frac{1}{10}A_2$$

Transverse polarisation

$$< \sin\theta \ \cos\phi >= \frac{1}{4}A_3$$

Product of V-A couplings, sensitive to the Weinberg angle

$$< \cos\theta >= \frac{1}{4}A_4$$

8/3*A_{FB}, non-zero at LO

$$< \sin^2\theta \ \sin 2\phi >= \frac{1}{5}A_5$$

$$< \sin 2\theta \ \sin\phi >= \frac{1}{5}A_6$$

$$< \sin\theta \ \sin\phi >= \frac{1}{4}A_7$$

Zero at NLO, first contributions at NNLO

$$\left\langle P\left(\cos\theta,\phi\right)\right\rangle = \frac{\int P(\cos\theta,\phi)\, d\sigma(\cos\theta,\phi)\, d\cos\theta\, d\phi}{\int d\sigma(\cos\theta,\phi)\, d\cos\theta\, d\phi}$$

A_{FB}

$$\sigma_F = \int_0^1 \frac{d\sigma}{d\cos\theta} d\cos\theta \quad , \quad \sigma_B = \int_{-1}^0 \frac{d\sigma}{d\cos\theta} d\cos\theta$$

$$A_{FB} = \frac{\sigma_F - \sigma_B}{\sigma_F + \sigma_B}$$

The angle θ is defined as the direction between the incoming quark and the lepton in the final state.
In pp collisions, the c.o.m. frame is unobservable.

At the LHC we can observe the reconstructed AFB*

At LO the direction of the incoming quark is defined by the boost of the di-lepton system.

At NLO the angle is defined in the Collins-Soper frame.

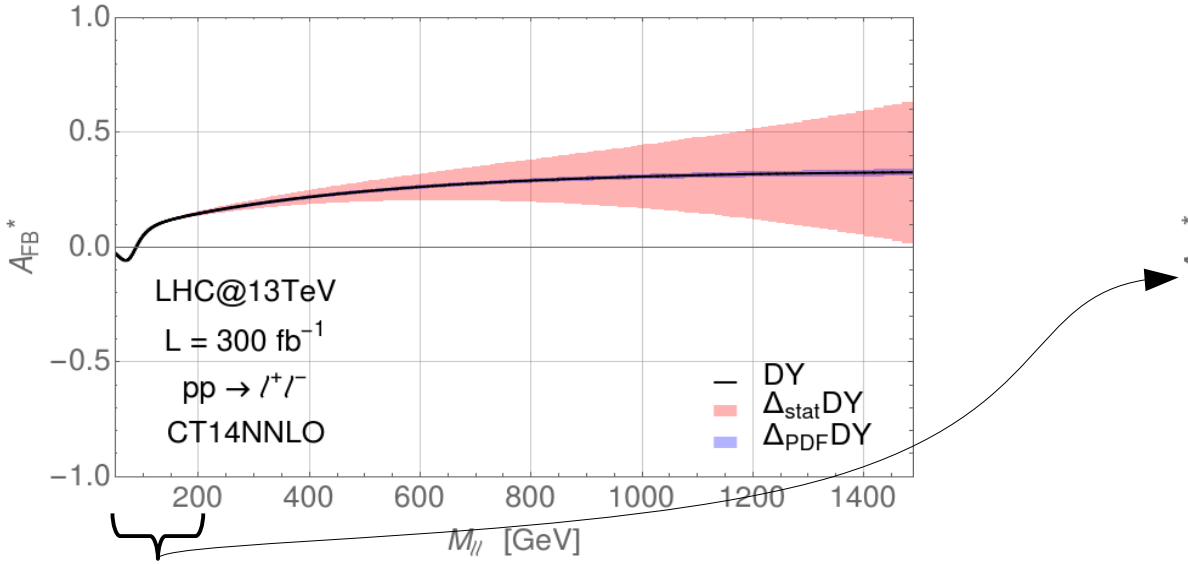

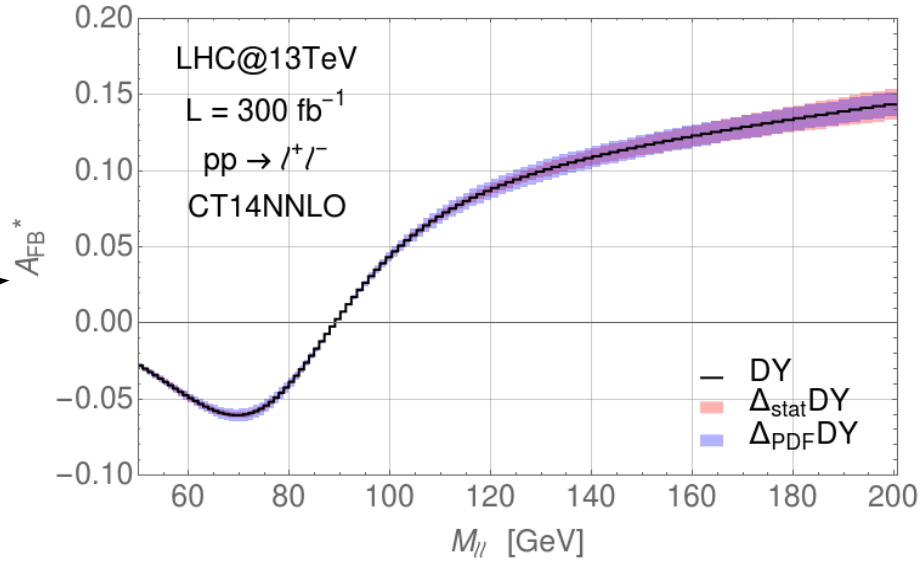

AFB has smaller systematic but larger statistical error compared to cross section measurements.

- High-invariant mass region: dominated by statistical uncertainties.
- Z peak region: high-stats to perform very precise measurements.

Neutral channel asymmetry

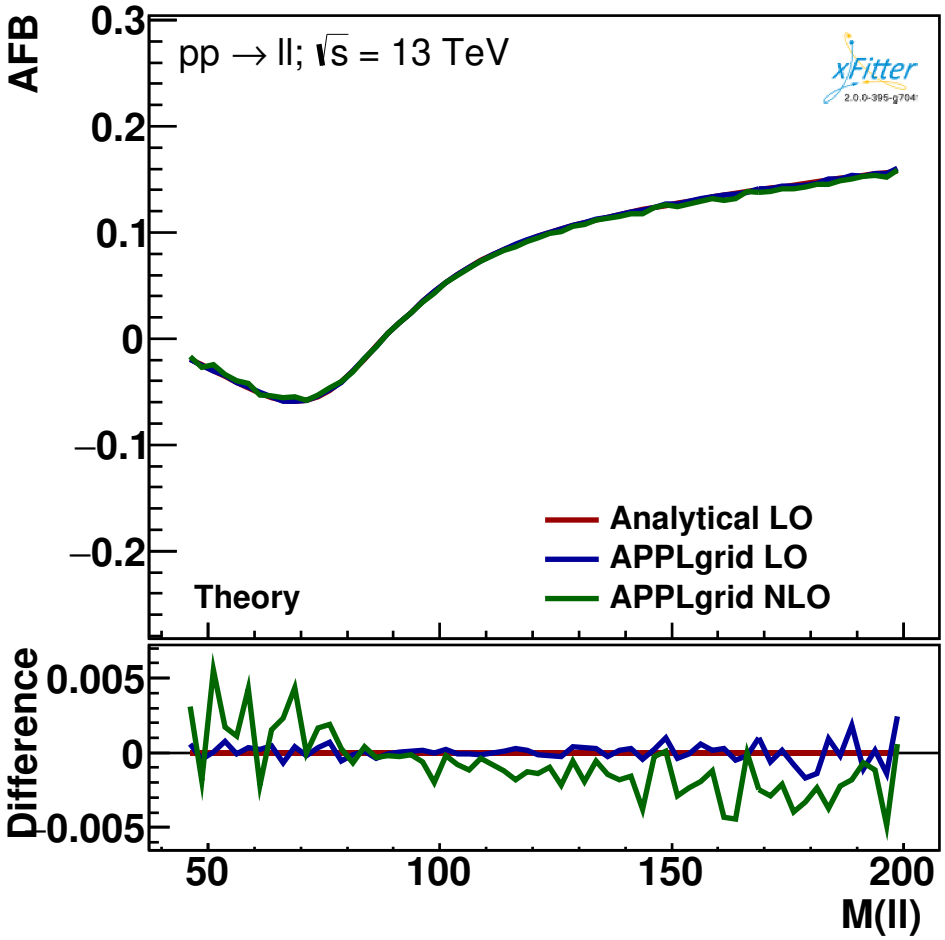

Radiative corrections are small.

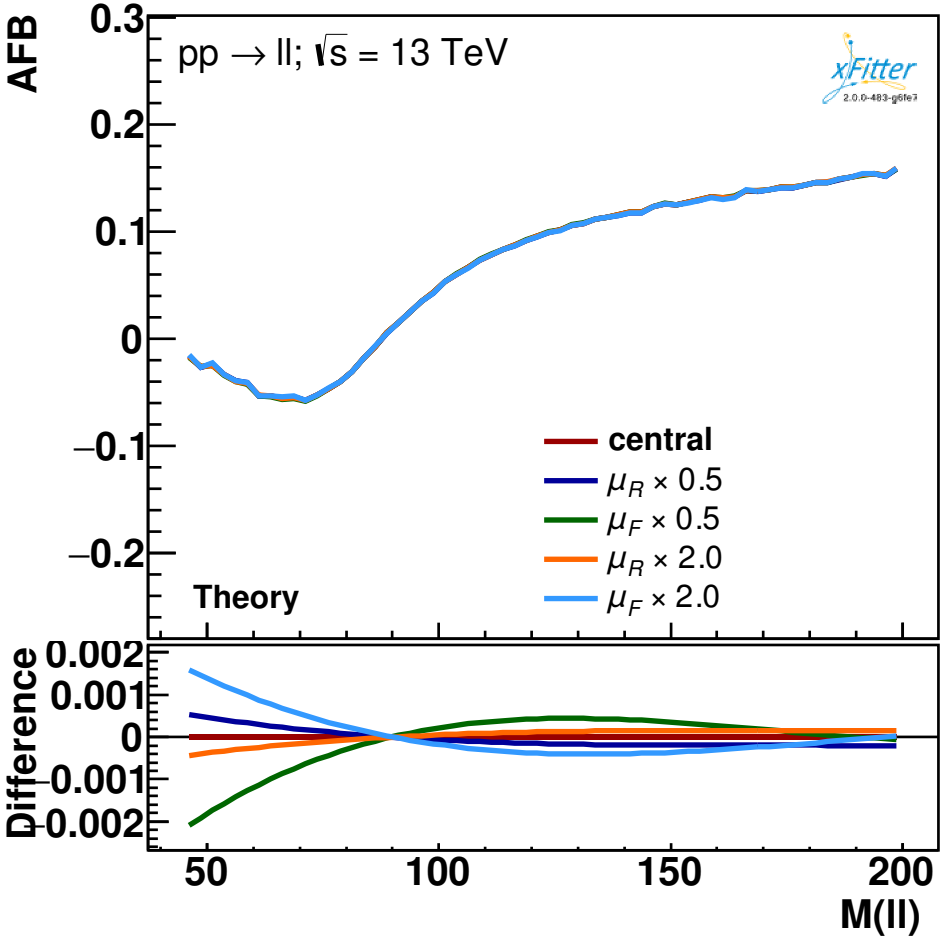

Theory uncertainty from scale variation under control.

A_{FB} and $\sin^2\theta_W$

- Theoretical uncertainty from the employed value of $\sin^2\theta_W$
- Most accurate measurement from LEP and SLD data: $\Delta\sin^2\theta_W = 16 \times 10^{-5} \rightarrow |\Delta A_{FB}| < 10^{-4}$

  Phys.Rept. 427 (2006) 257-454
- Most accurate prediction from EW global fit: $\Delta\sin^2\theta_W = 6 \times 10^{-5} \rightarrow |\Delta A_{FB}| < 4 \times 10^{-5}$

  Eur.Phys.J.C 78 (2018) 8, 675
- Some differences in the profiled curves
- Deviations of A_{FB} generally small compared to statistical or other systematical uncertainties

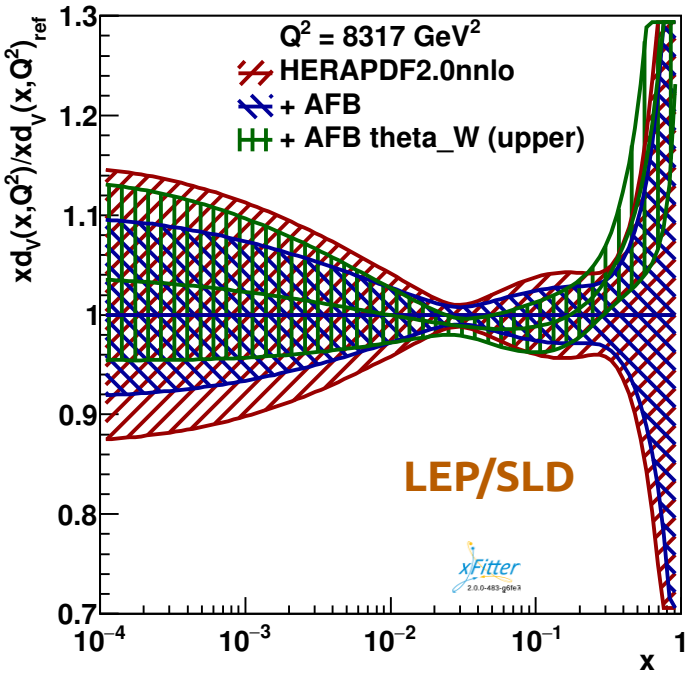

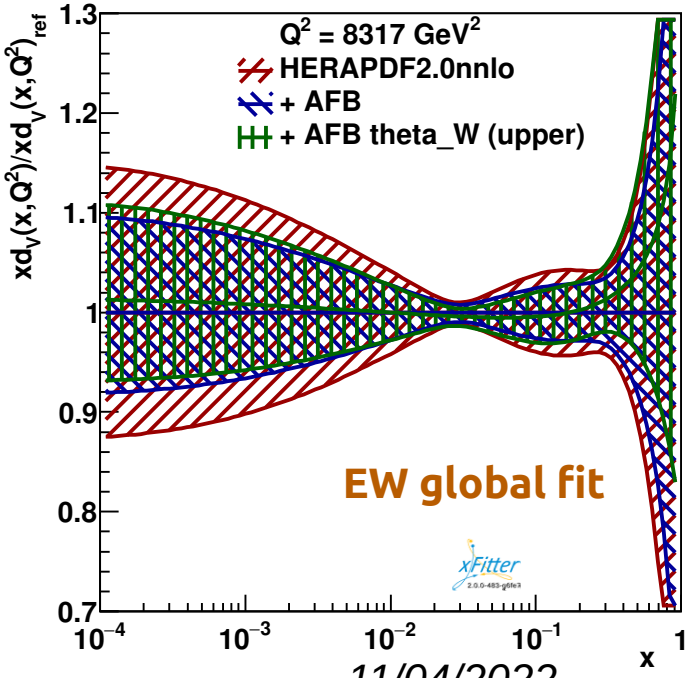

PDFs and $\sin^2\theta_W$

- Extraction of $\sin^2\theta_{eff}$ is performed through A_{FB} measurements.
- PDFs are the main source of uncertainty.
- Ongoing studies by LHC-EW-WG to provide different global fits and correlations between PDF sets.

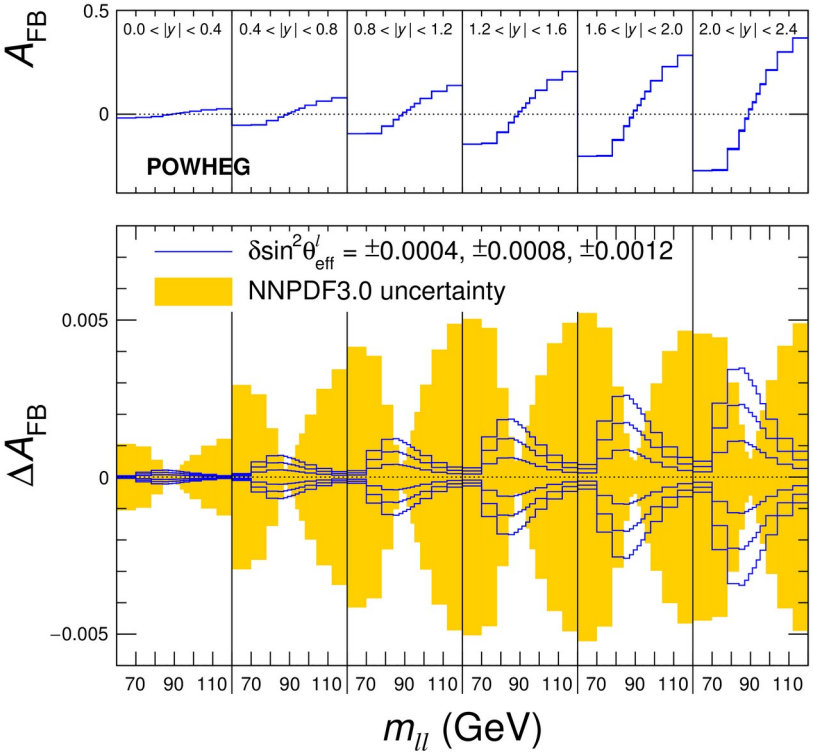

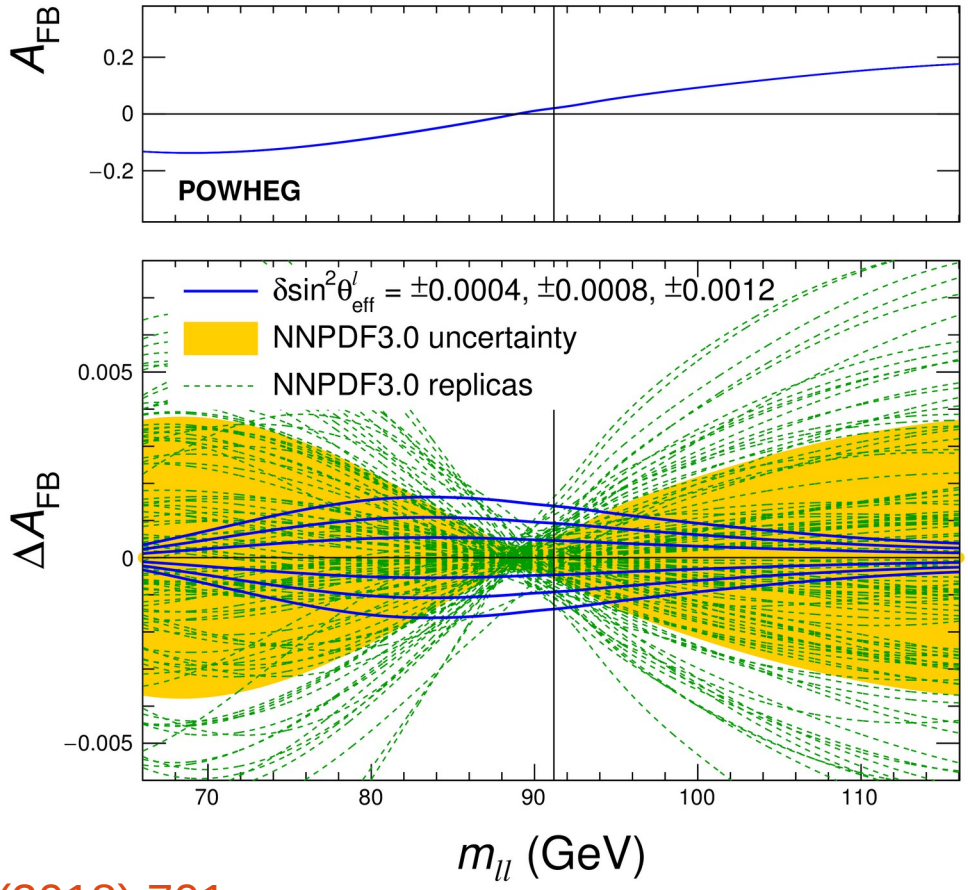

EPJC 78 (2018) 701

A_{FB} eigenvector rotation

Assess the single PDF sensitivity on A_{FB} data through eigenvector rotation exercise:

J. Pumplin, Phys. Rev. D 80 (2009) 034002

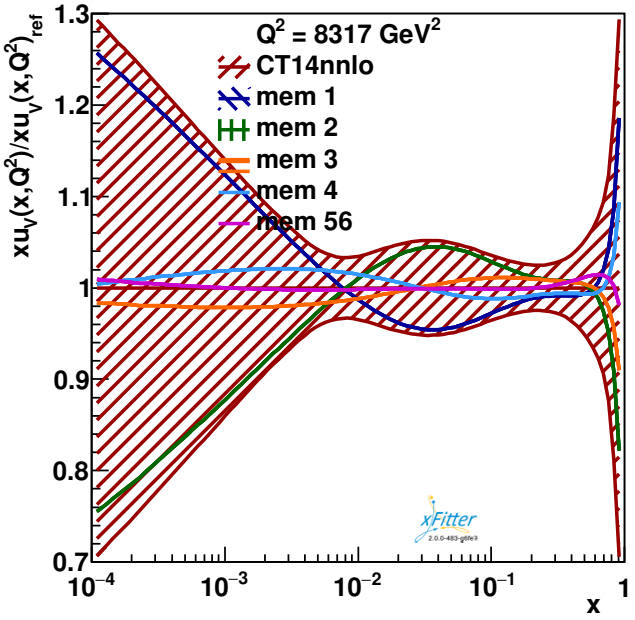

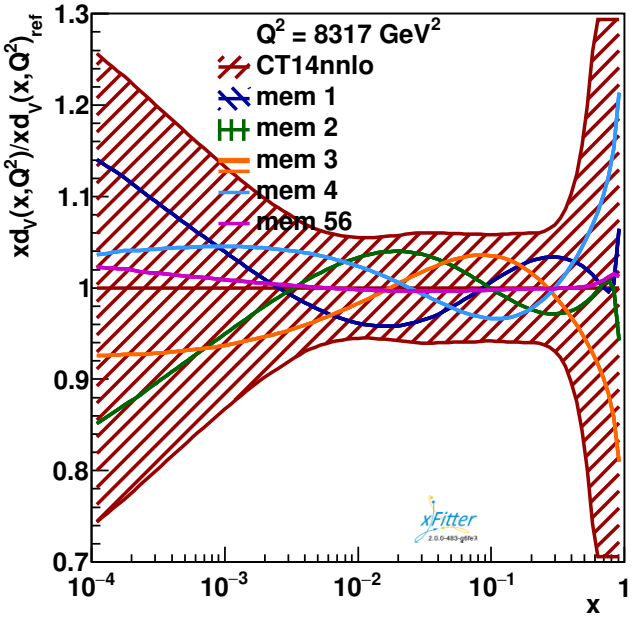

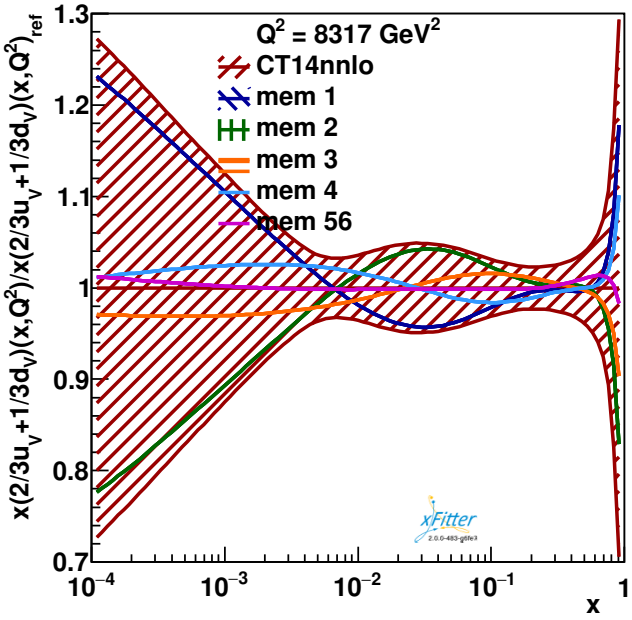

- Eigenvectors rotated and sorted according to their sensitivity to the new data.
- First pair or eigenvectors almost completely saturate the error bands.
- Largest sensitivity on valence quarks, particularly on the combination **(1/3 d_V +2/3 u_V)**

Lepton-charge asymmetry

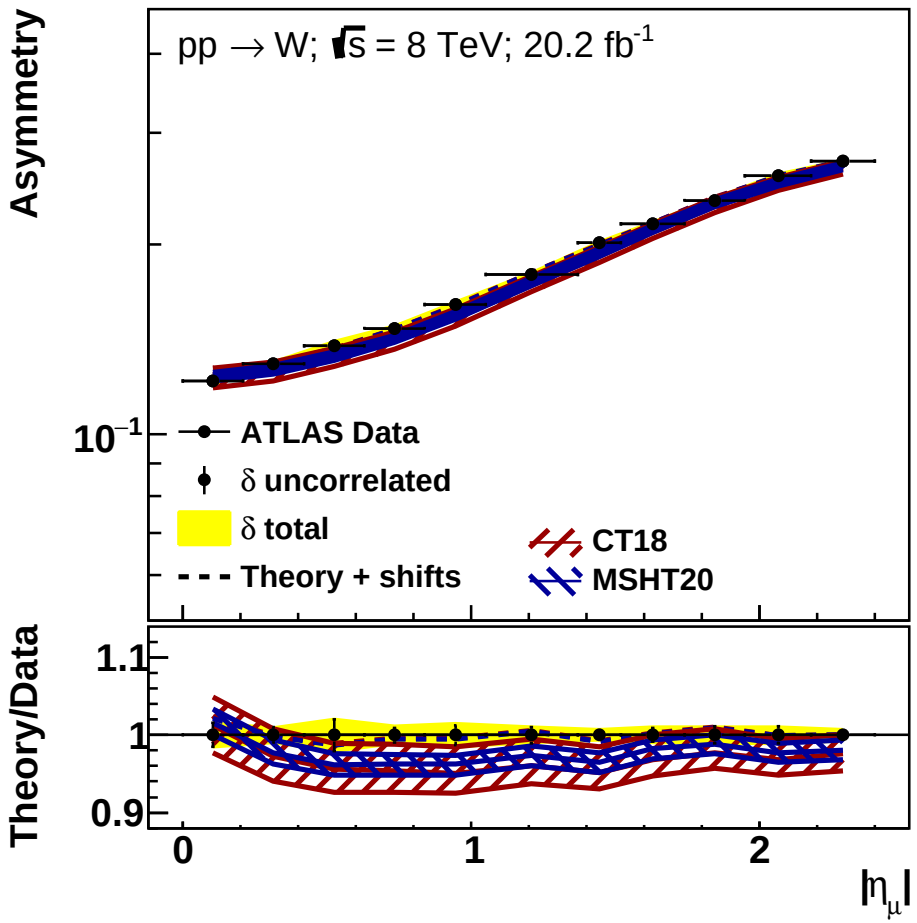

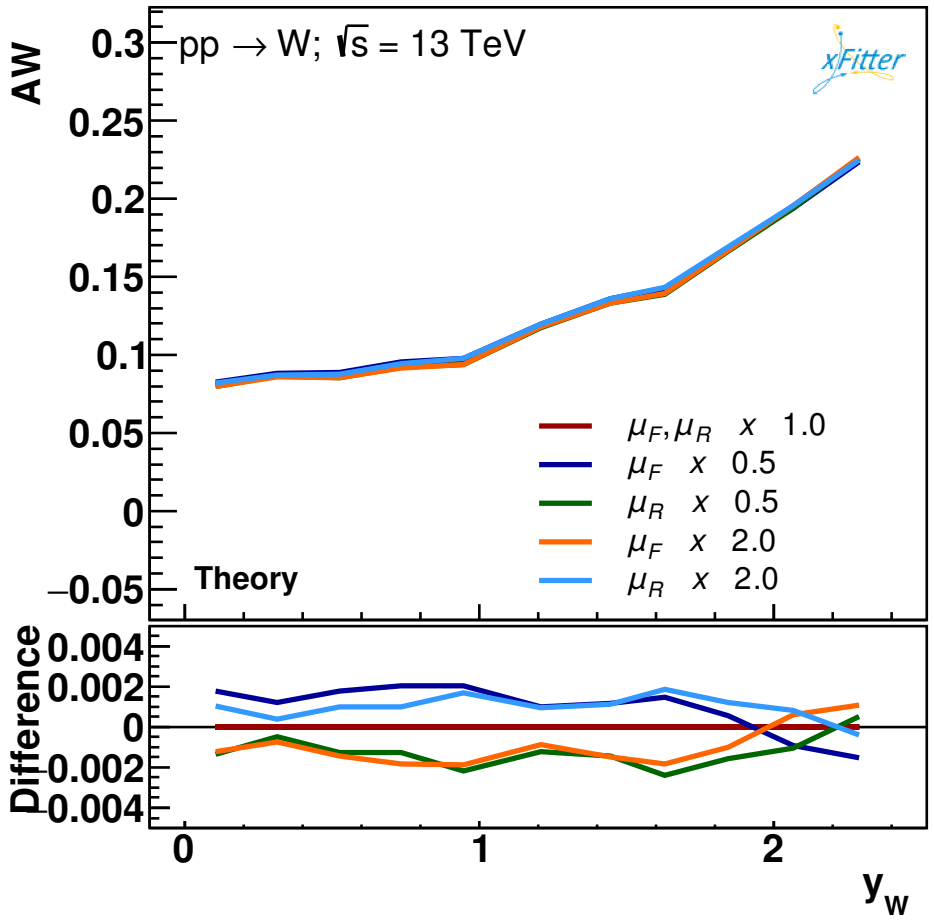

Theory uncertainty from scale variation under control, well below PDF uncertainties.

A_W eigenvector rotation

Assess the single PDF sensitivity on A_W data through eigenvector rotation exercise:

J. Pumplin, Phys. Rev. D 80 (2009) 034002

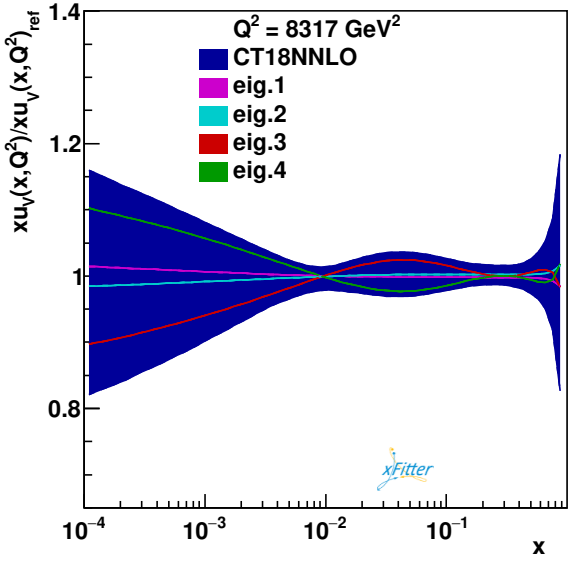

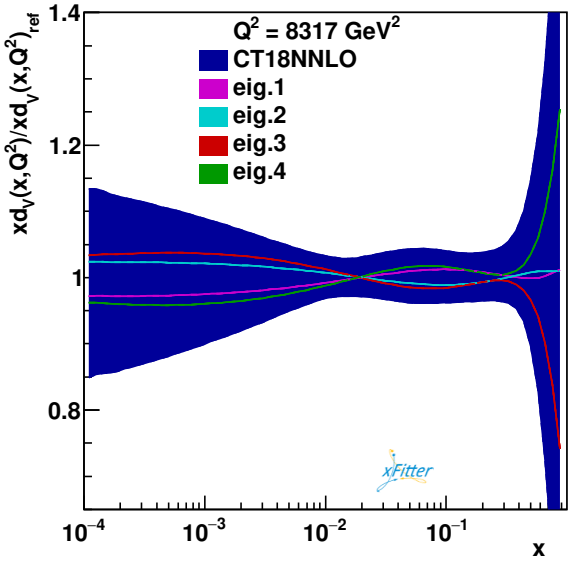

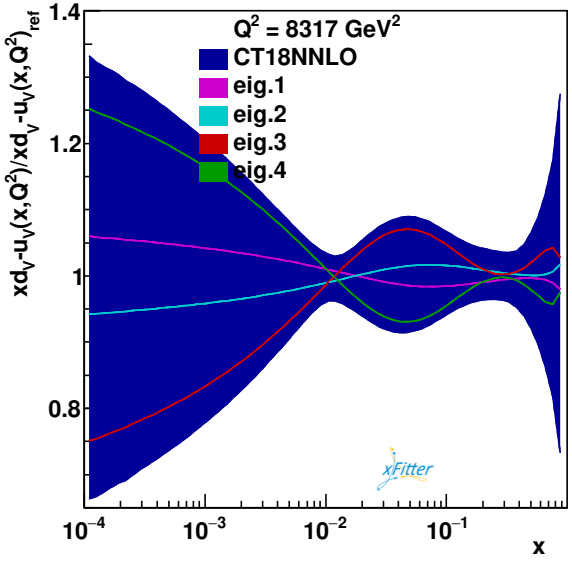

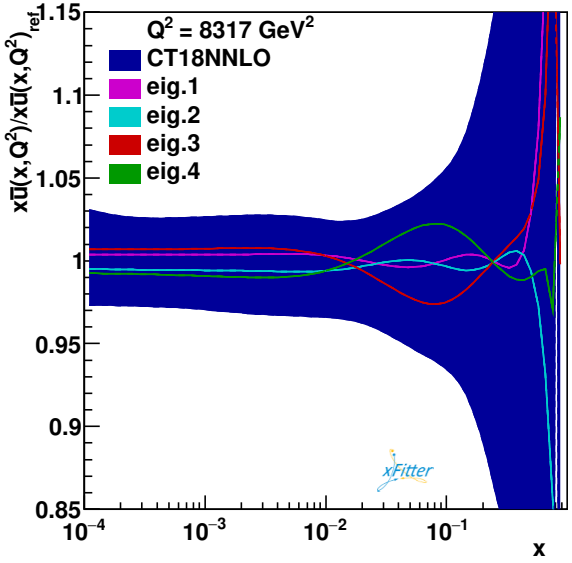

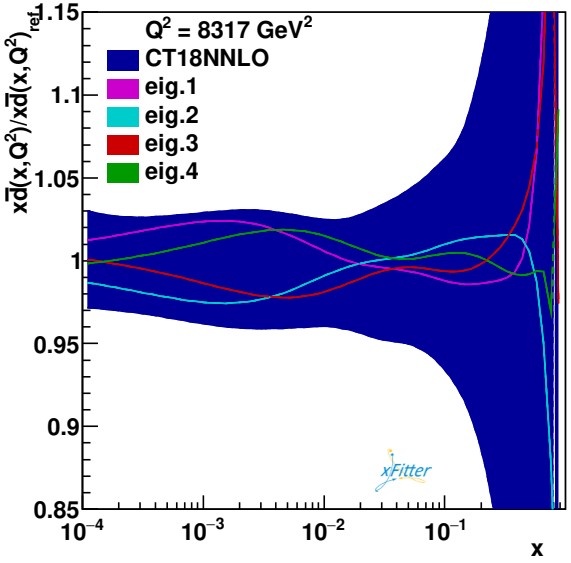

Largest sensitivity on valence quarks, particularly on the combination **($d_V - u_V$)**

Complementarity with A_{FB} most sensitive to **(1/3 d_V +2/3 u_V)**

A_W vs A_{FB}

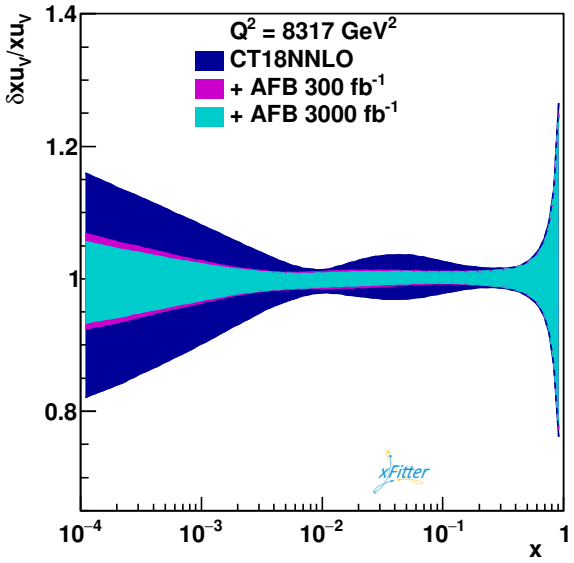

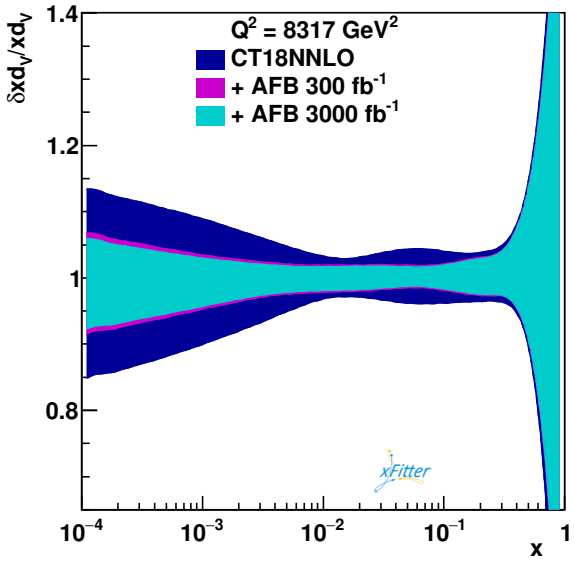

CT18NNLO + A_{FB}

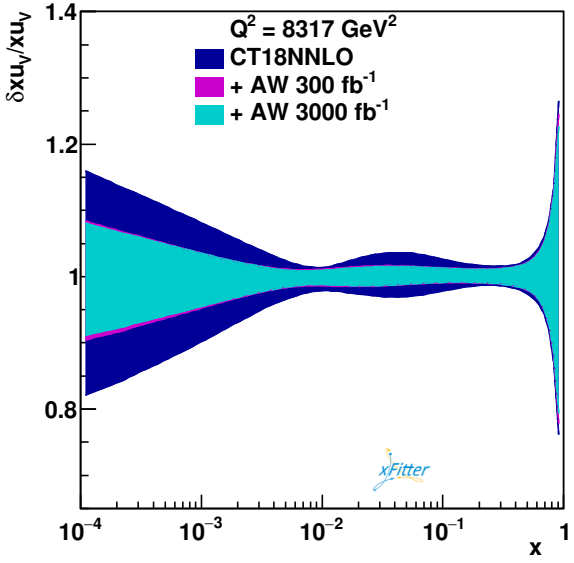

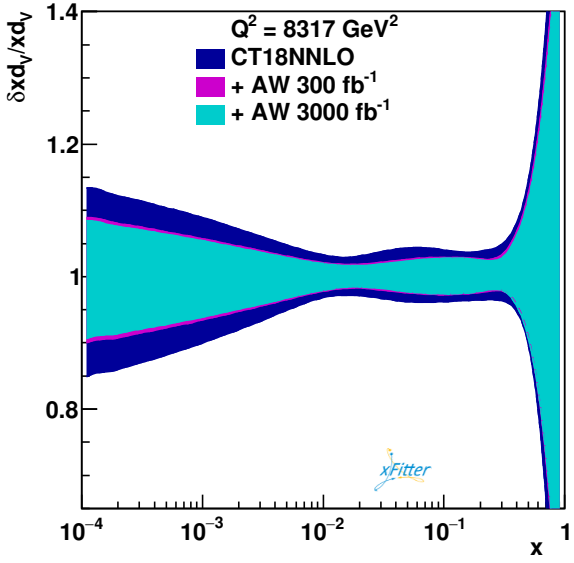

CT18NNLO + A_W

Comparable sensitivity on valence quark PDFs, with **A_{FB}** providing slightly stronger constraints.

Saturation of uncertainty reduction from 300 fb^{-1} to 3000 fb^{-1}.

A_W vs A_{FB}

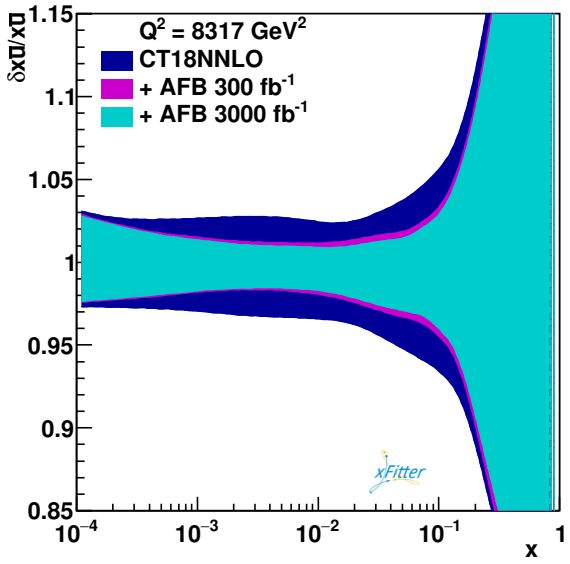

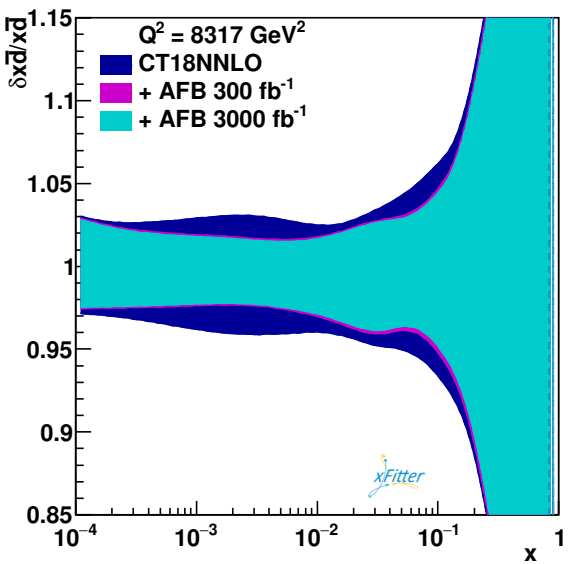

CT18NNLO + A_{FB}

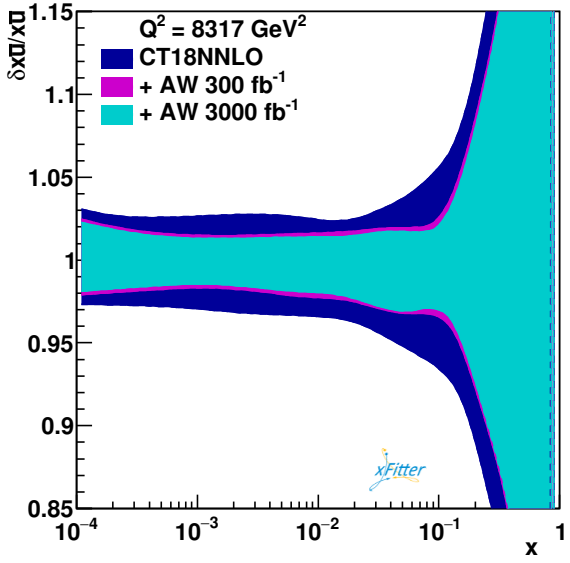

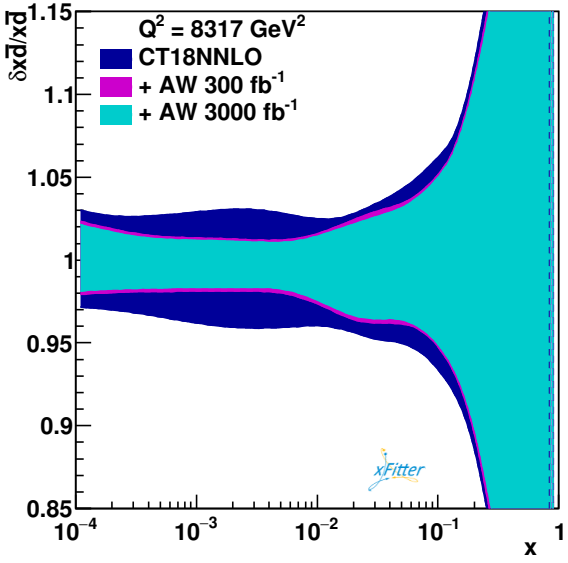

CT18NNLO + A_W

A_W provides slightly stronger than **A_{FB}** on anti-quark PDFs, particularly for $\bar{u}$ in the low x region and for $\bar{d}$ in the low and intermediate x range.

Impact on M_W determination

Reduction of PDF uncertainties crucial for SM precision measurements.

Lepton + MET transverse mass spectrum for extraction of M_W

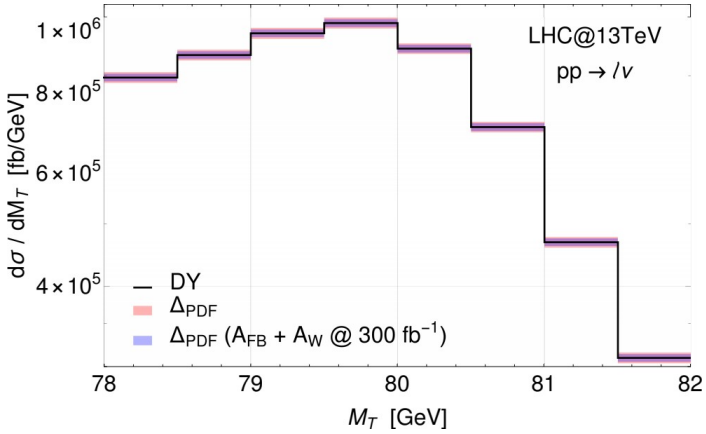

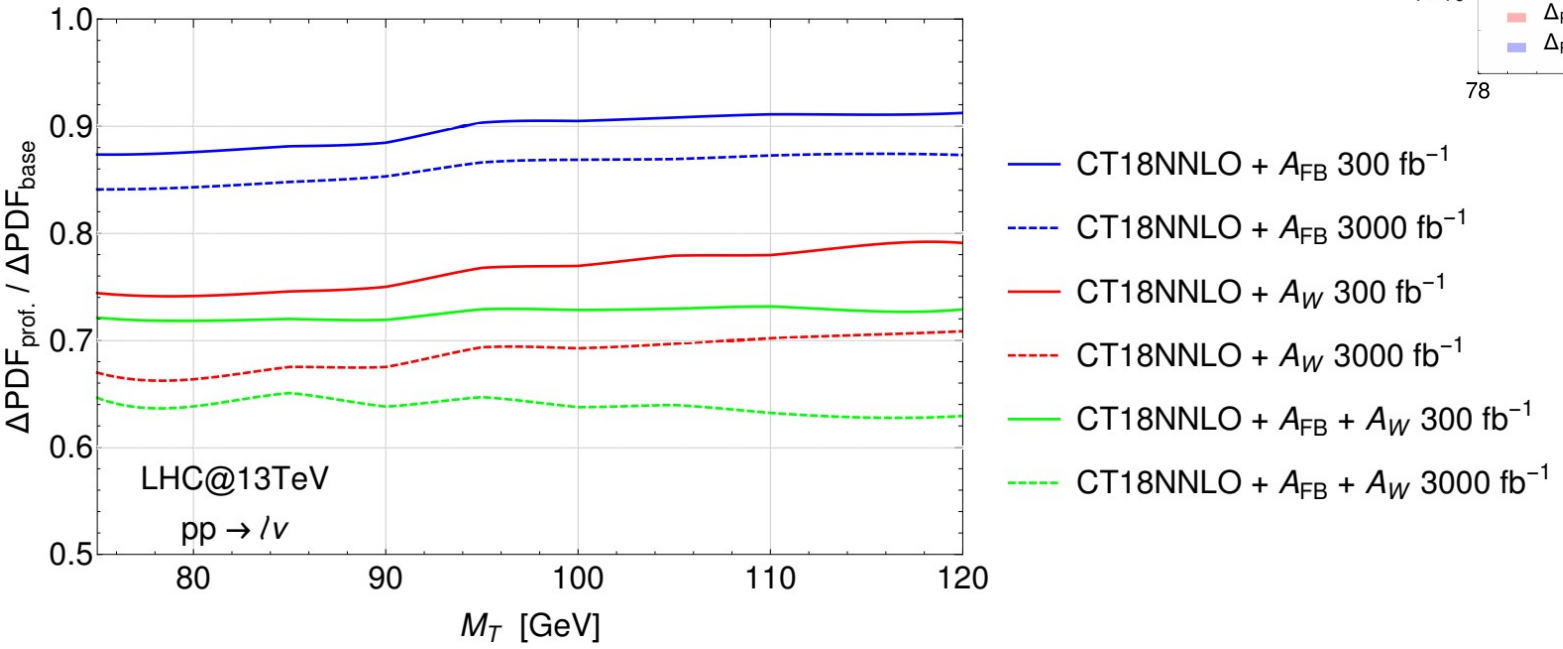

PDF uncertainty before profiling about 1.8%

- **A_{FB}** 300 (3000) fb^{-1} data reduces PDF uncertainty ~ 12% (~16%)
- **A_W** 300 (3000) fb^{-1} data reduces PDF uncertainty ~26% (43%)
- Combination of **A_{FB}** and **A_W** 300 (3000) fb^{-1} reduces PDF uncertainty ~28% (~46%)

(REMARK: assessing the improvement on M_W measurement requires a delicate and refined analysis of normalized distribution, where reduction of uncertainty is far more moderate)

A_W for proton antimatter asymmetry

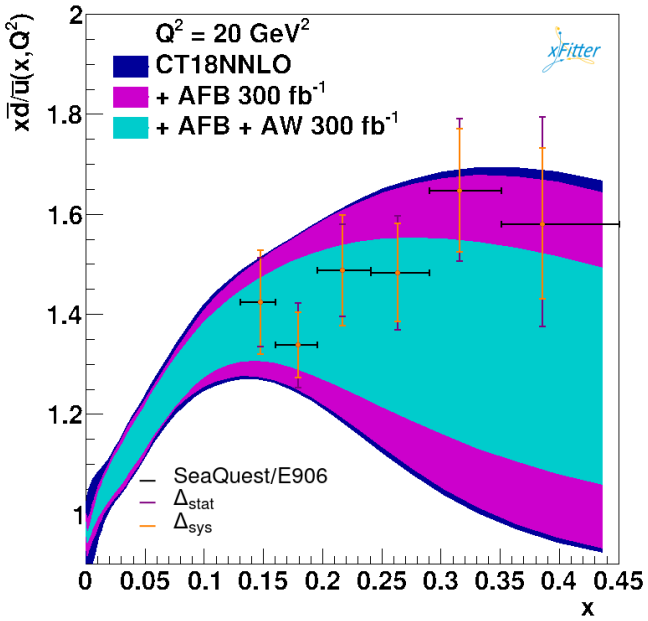

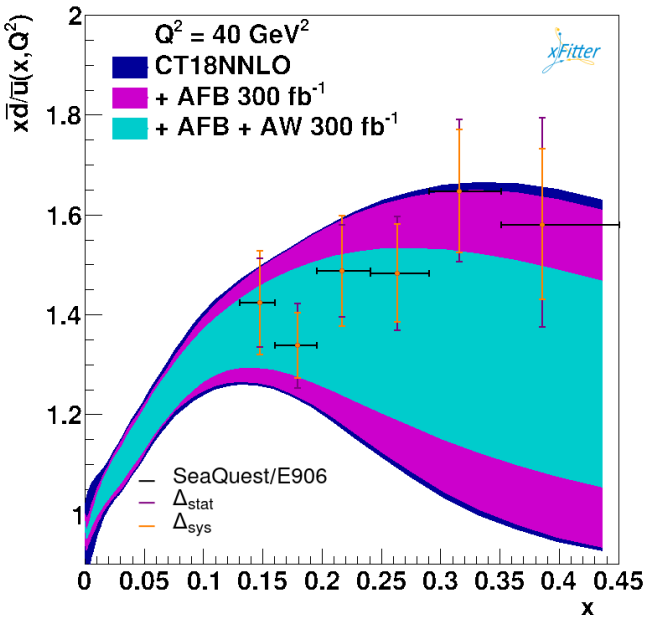

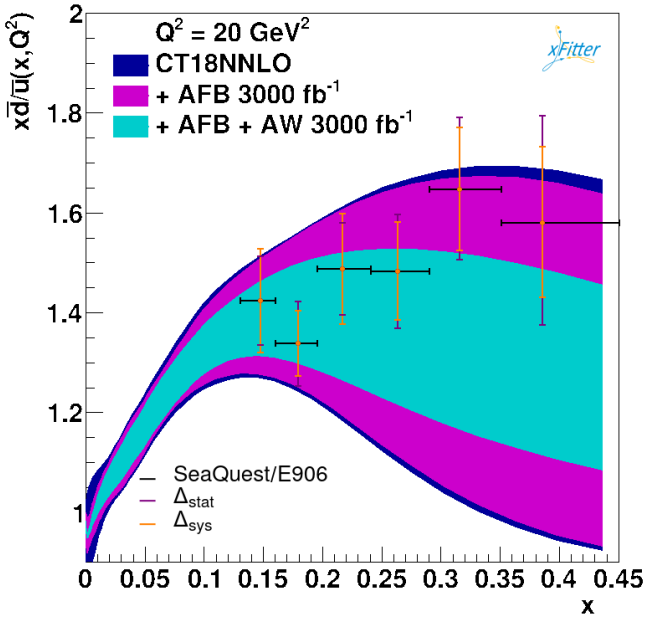

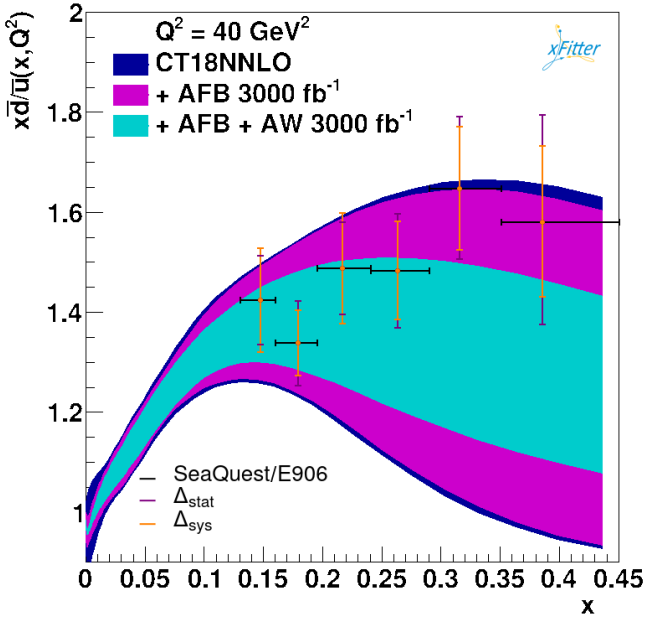

SeaQuest Collaboration, Nature 590 (2021) 7847, 561-565

Uncertainties in the neutral channel

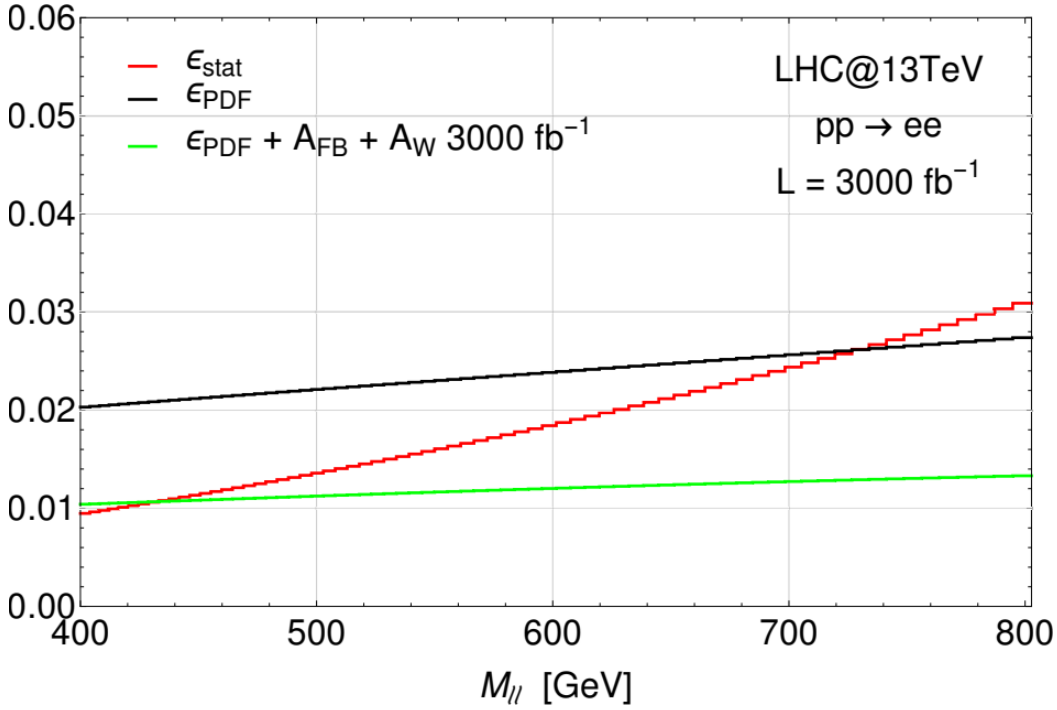

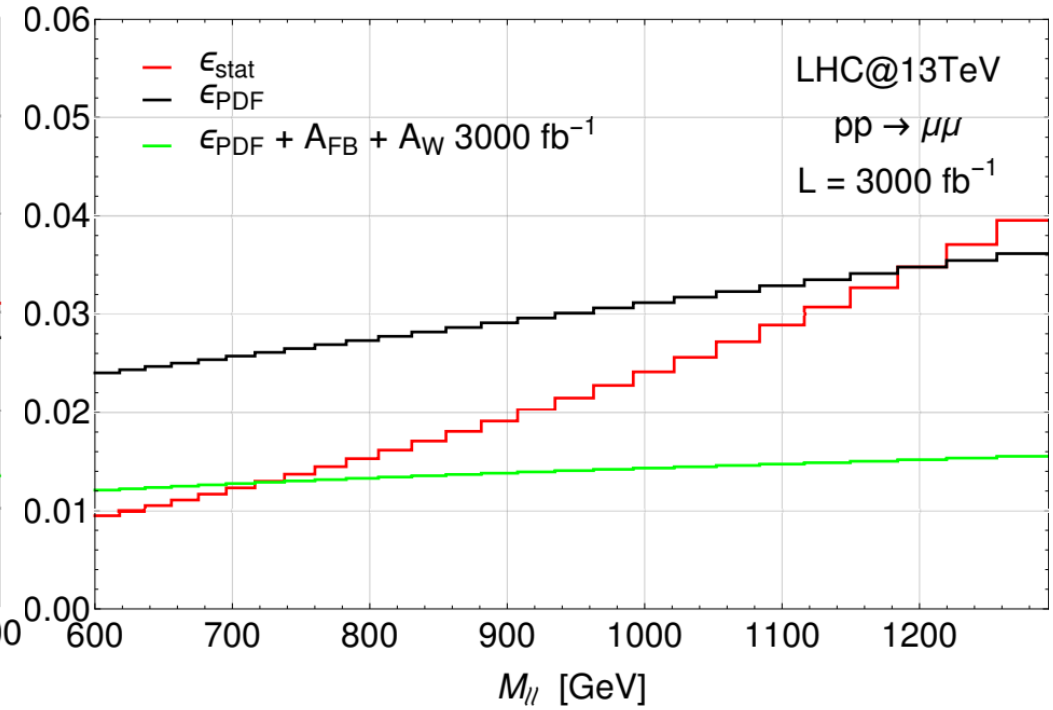

The improvement on PDF determination increases the sensitivity to BSM physics and enables the diagnostic power of experimental analysis.

Effects on *Z'* searches

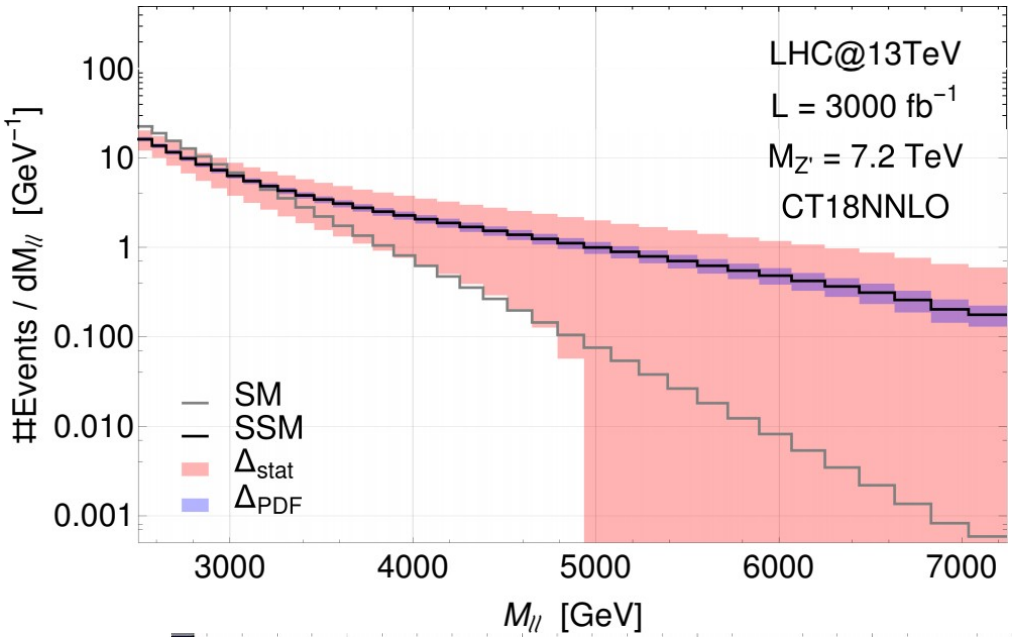

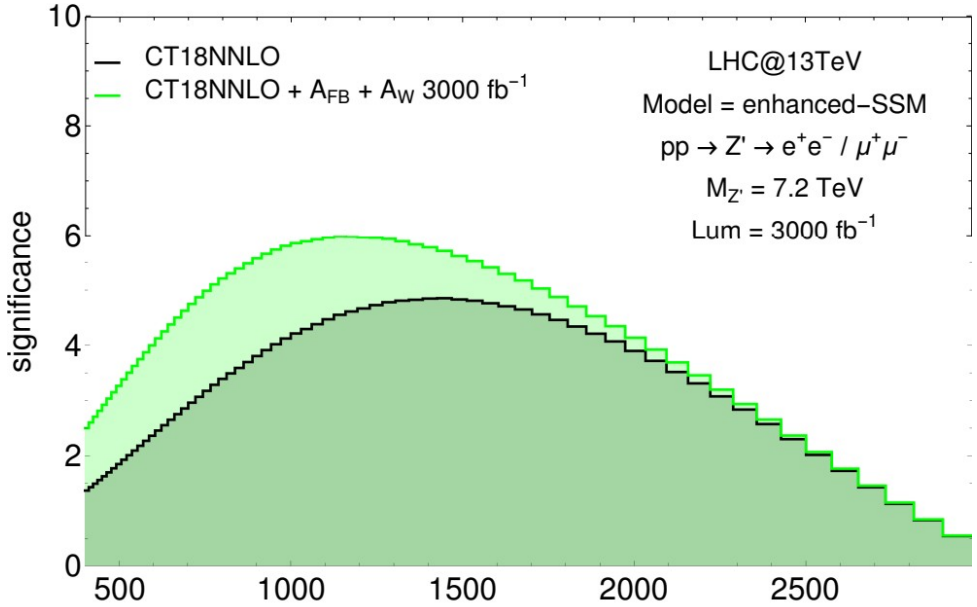

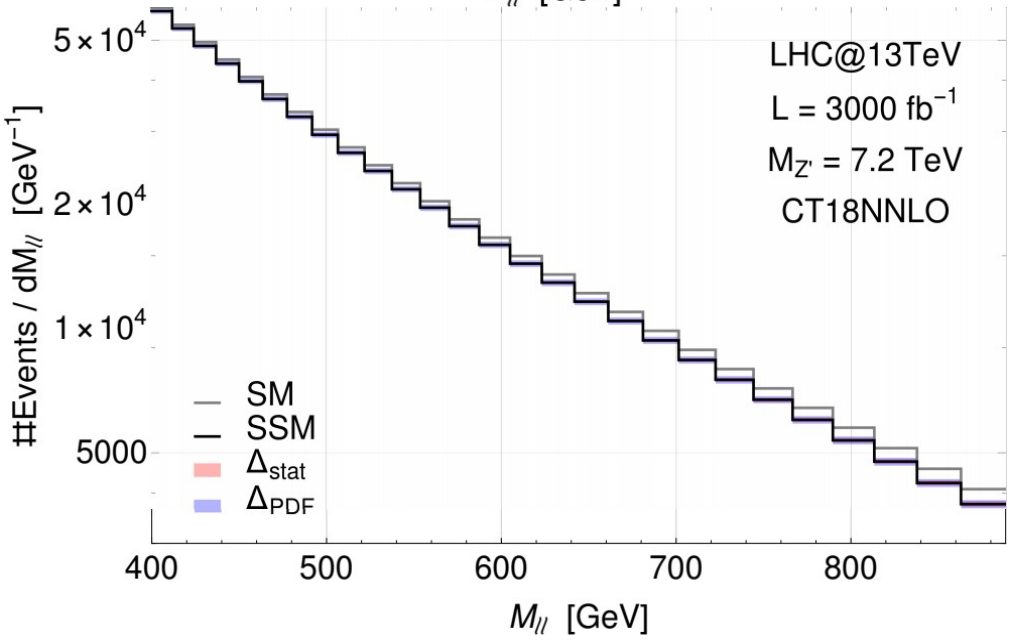

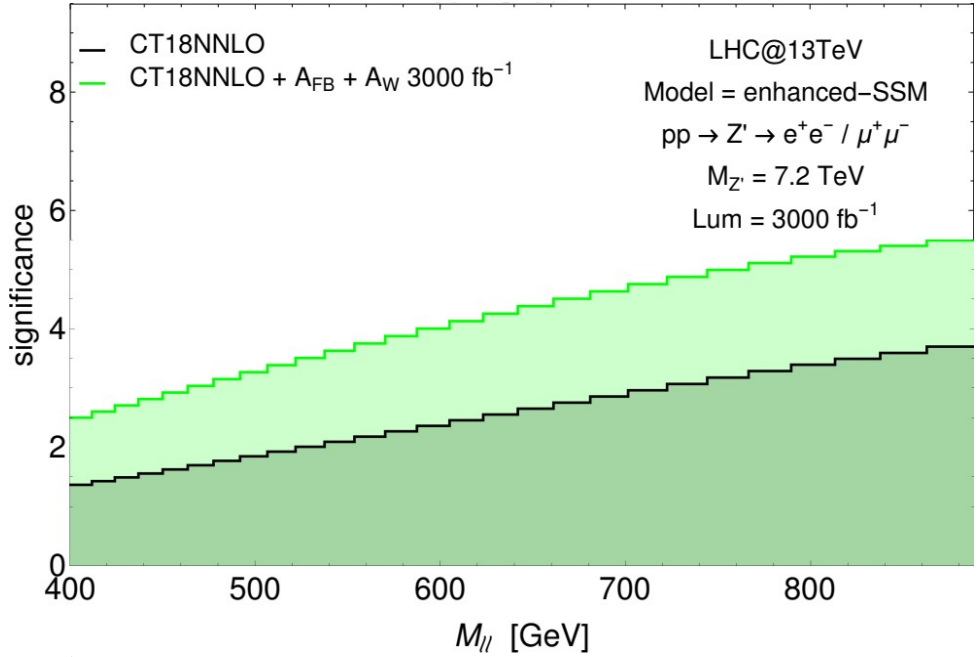

Z' from enhanced SSM

Uncertainties in the charged channel

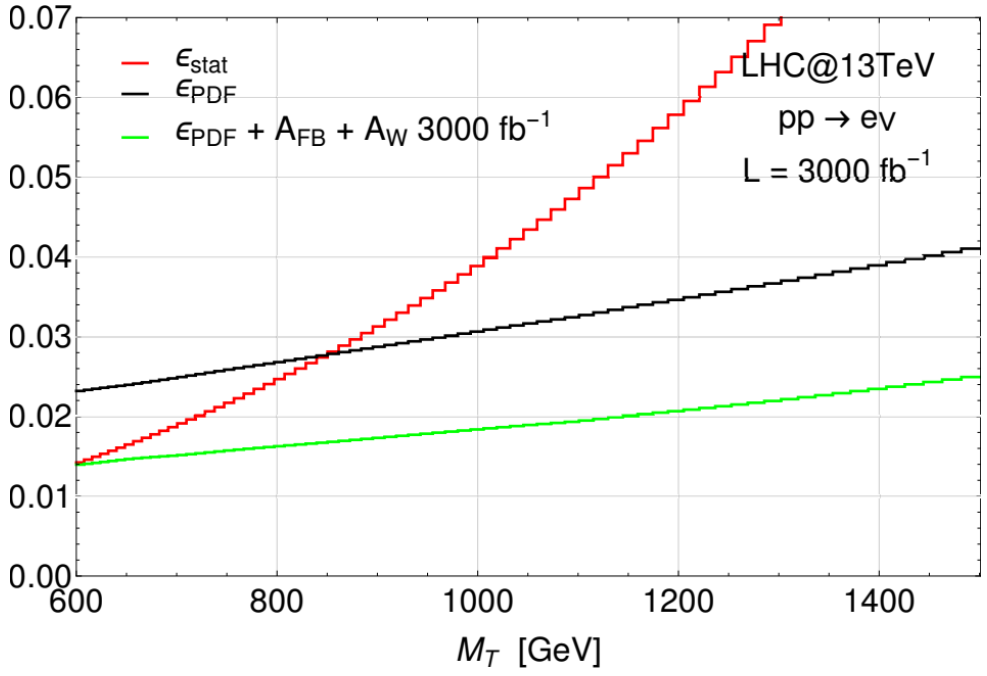

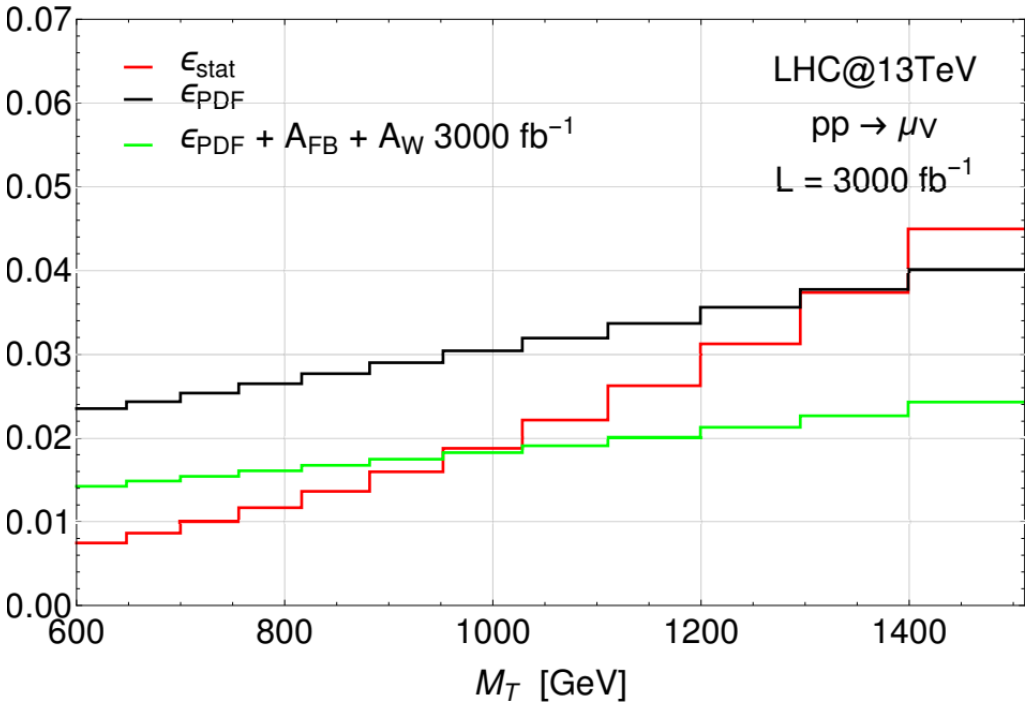

The improvement on PDF determination increases the sensitivity to BSM physics and enables the diagnostic power of experimental analysis.

Effects on *W'* searches

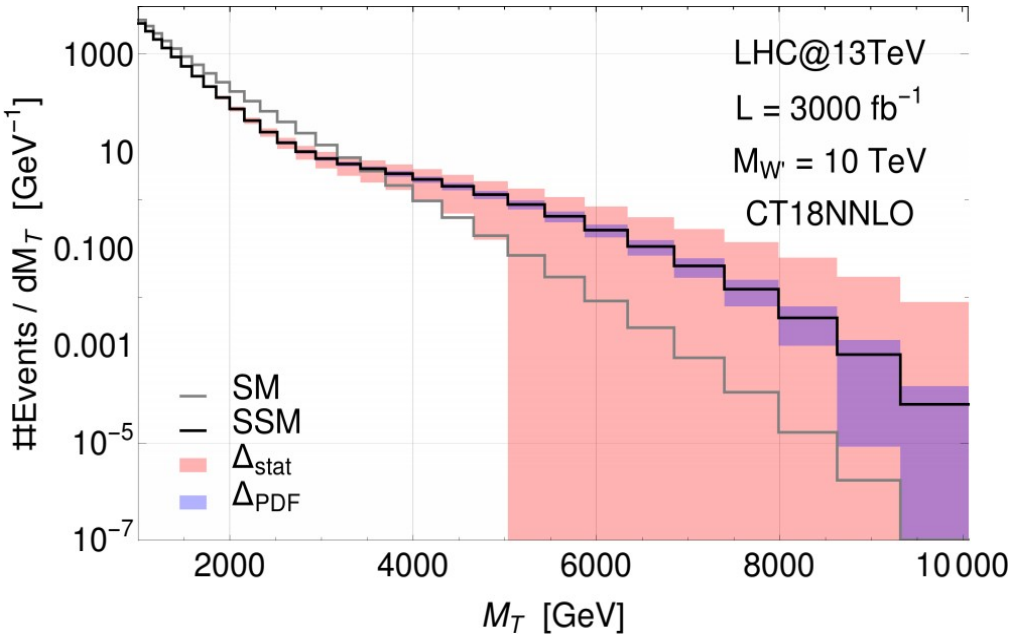

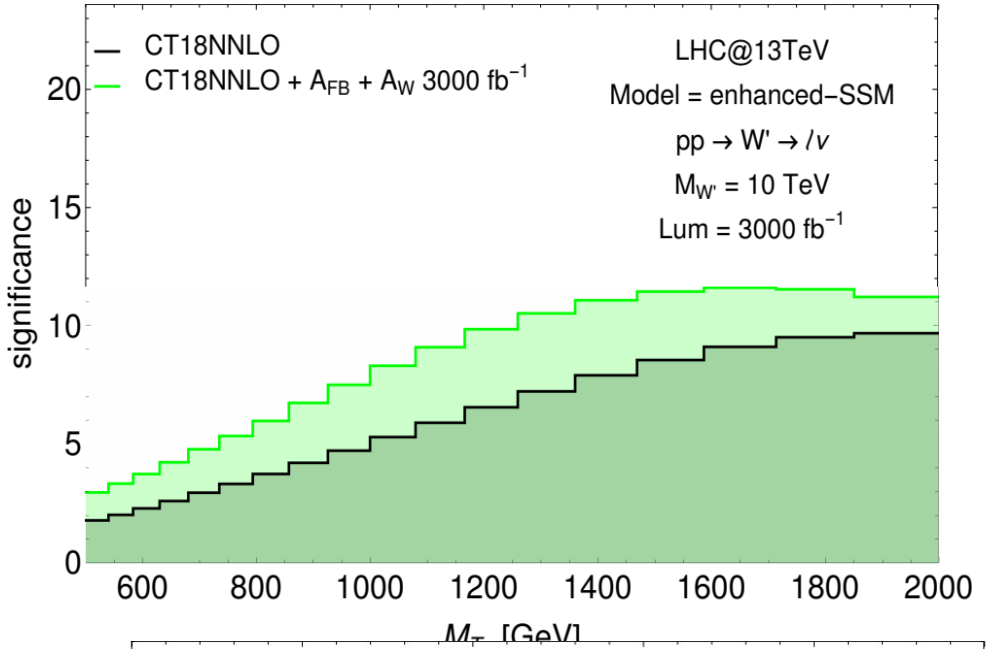

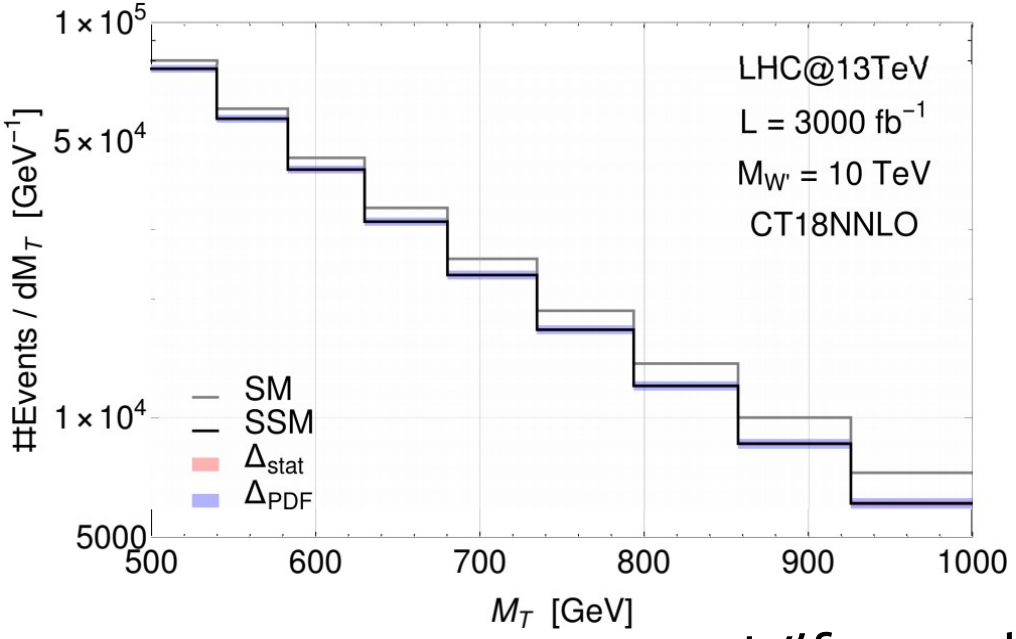

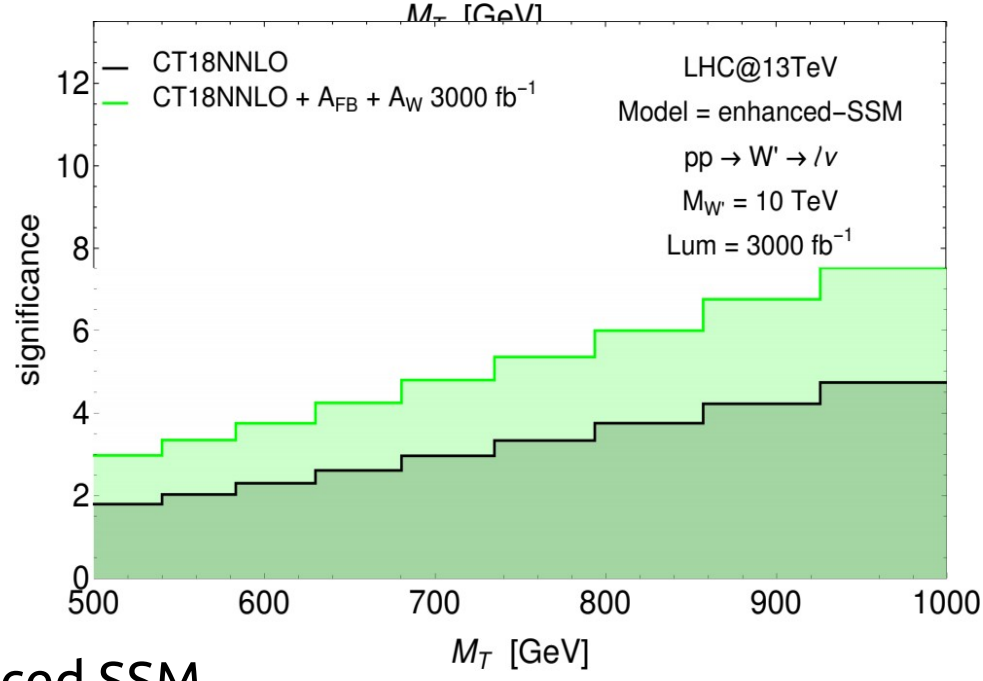

W' from enhanced SSM

BSM high mass searches

Significant reduction of uncertainties in the high transverse/invariant mass spectra for BSM searches.

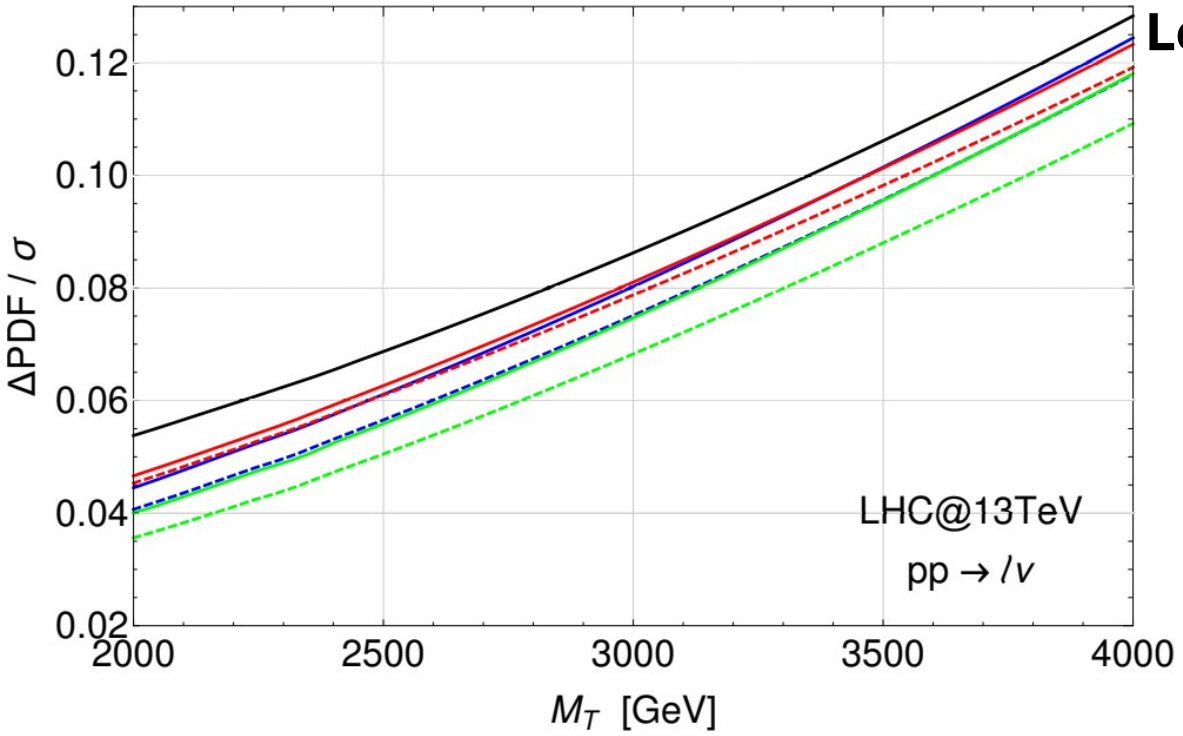

Lepton + MET high transverse mass:

- CT18NNLO
- CT18NNLO + A_{FB} 300 fb^{-1}
- CT18NNLO + A_{FB} 3000 fb^{-1}
- CT18NNLO + A_W 300 fb^{-1}
- CT18NNLO + A_W 3000 fb^{-1}
- CT18NNLO + A_{FB} + A_W 300 fb^{-1}
- CT18NNLO + A_{FB} + A_W 3000 fb^{-1}

Original PDF uncertainty (i.e.) at 4 TeV from 12.9% is reduced to:

- 12.5% (11.8%) by $\mathbf{A_{FB}}$ 300 (3000) fb^{-1} data
- 12.3% (11.9%) by $\mathbf{A_W}$ 300 (3000) fb^{-1} data
- 11.8% (10.9%) by combination of $\mathbf{A_{FB}}$ and $\mathbf{A_W}$ 300 (3000) fb^{-1} data

BSM resonances detection

PDF uncertainties are relevant in searches for non-resonant objects.

Benchmark: Enhanced SSM model
(same as SSM with BSM gauge coupling augmented by factor 3)

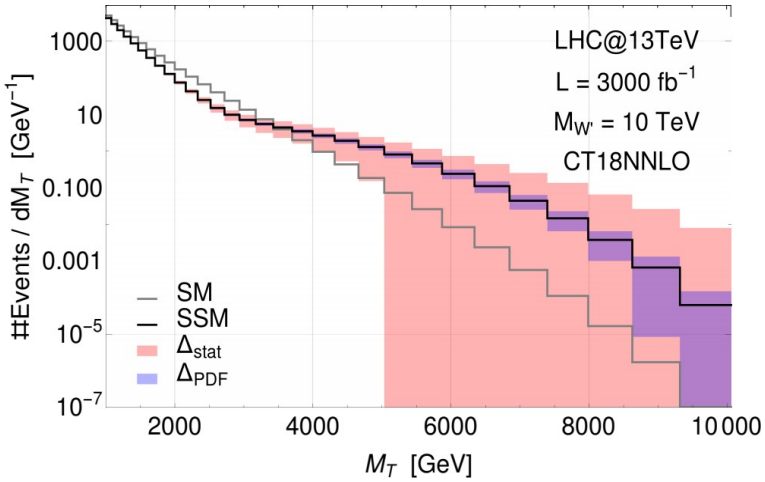

High transverse mass excess is non-significant

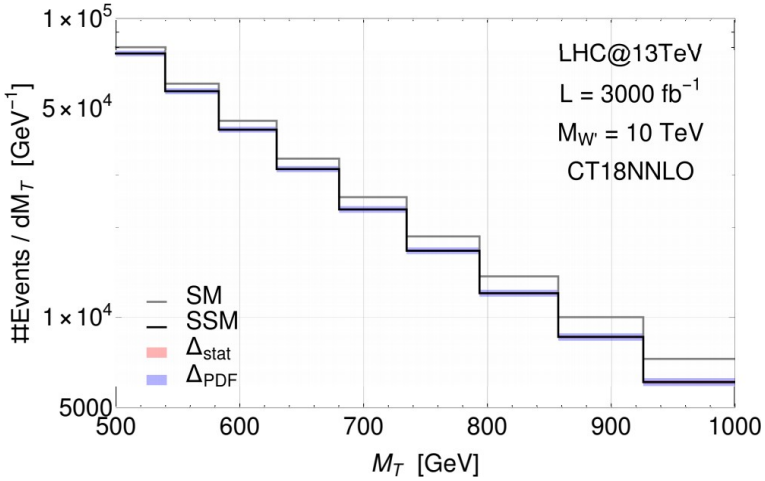

Significant depletion of events due to interference in the low transverse mass tail

Phys.Lett.B 803 (2020) 135293

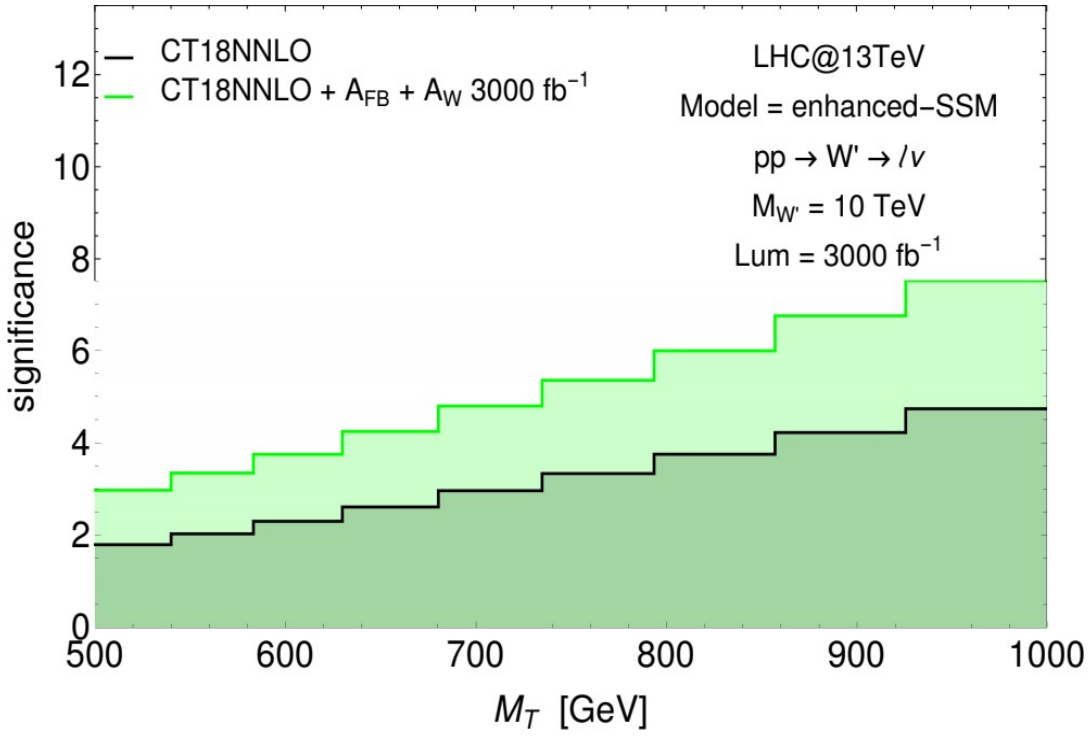

Early evidence of BSM physics significantly improved by reduction of PDF uncertainty

Case study: the 4DCHM

- **The Higgs boson is a bound state arising from a strong dynamics.**
  - The Higgs boson is a pseudo Naumbu-Goldstone boson from the breaking G → H
  - The most studied in the literature is the case of *SO(5) / SO(4)* Agashe, Contino, Pomarol, **Nucl. Phys. B719, (2005), 183**
- **The *SO(5) / SO(4)* coset:**
  - 4 Goldstone bosons.
  - Contains the SO(4) custodial symmetry to protect the parameter ρ.
  - *SO(5)* → *SO(4)* at the TeV scale.

- **The gauge sector described by two non linear σ-models.**
  - The introduction of the covariant derivative makes the two models interact: $SO(5)_L \otimes SO(5)_R \rightarrow SO(5)_{L+R} \rightarrow SO(4)$
  - In addition there is an extra *U(1)* which crosses the *SO(5)*. Son, Stephanov, **Phys. Rev. D69 (2004), 065020**
- **The degrees of freedom in the unitary gauge are:**
  - 10+1+4 scalars provided by the two σ-models.
  - 10+1 give mass to the 5 neutral and 6 charged spin 1 physical states.
  - The 4 left are identified with the SM Higgs sector d.o.f..
- **The particle content of the model is:**
  - **5 Z'** (only Z_2, Z_3 and Z_5 coupled to the SM)
  - **3 W'** (only W_2 and W_3 coupled to the SM)
- **Model parameters:**
  - New gauge coupling g_ρ
  - Compositness scale f
- **Gauge boson masses:**
  - For Z_2, Z_3 and W_2 roughly $m_\rho = f\, g_\rho$
  - For Z_5 and W_3 roughly $\sqrt{2} m_\rho$
  - Fine corrections proportional to $\xi = v^2 / f^2$ after the symmetries breaking.

BSM searches in the 4DCHM

Peak region

Dip region

Neutral channel

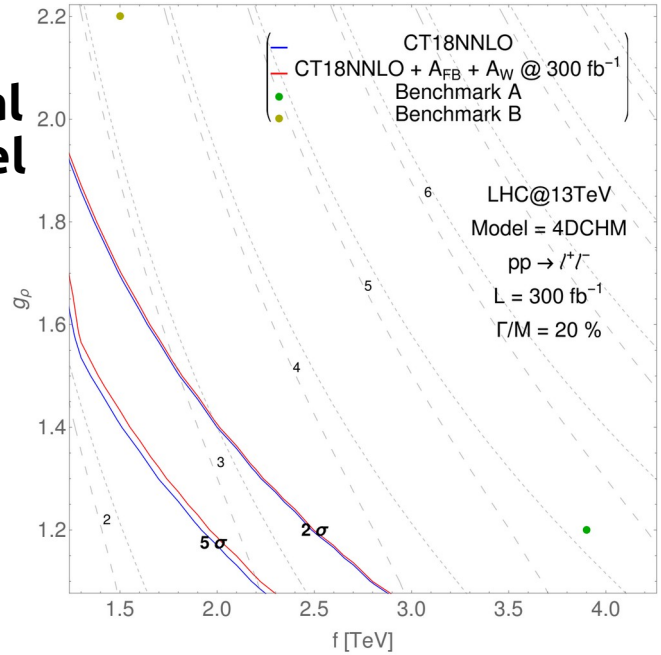

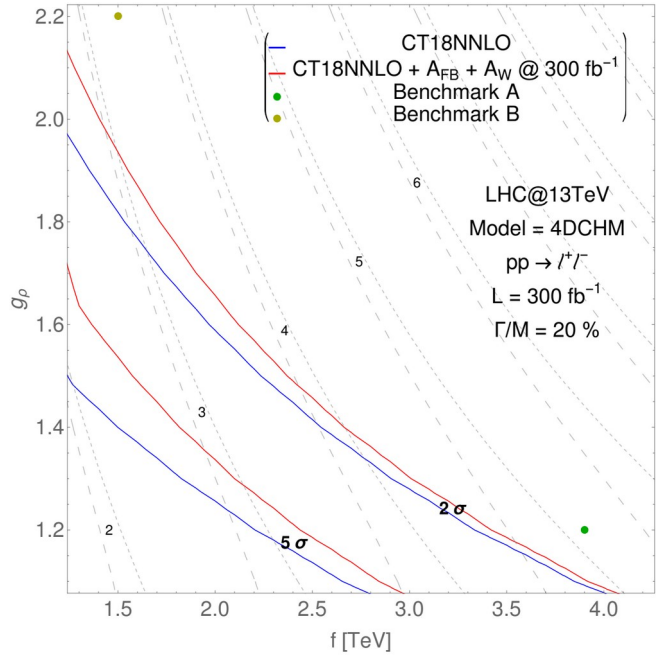

Charged channel

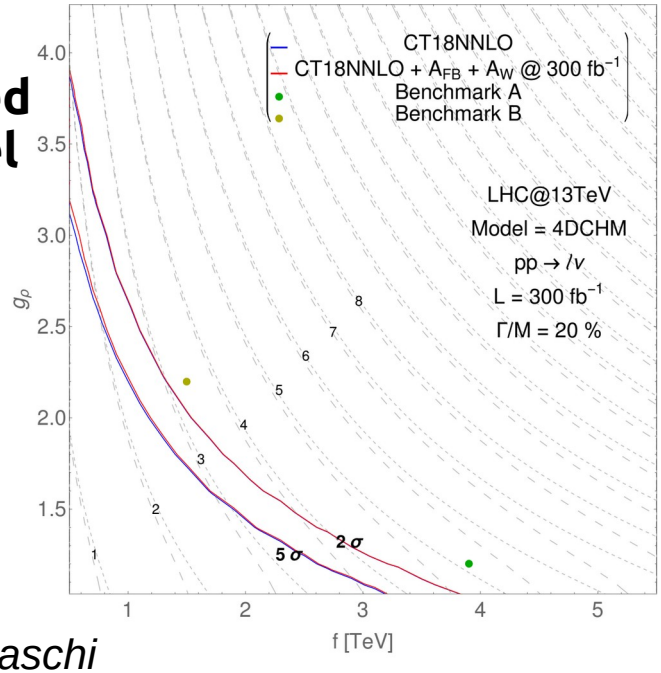

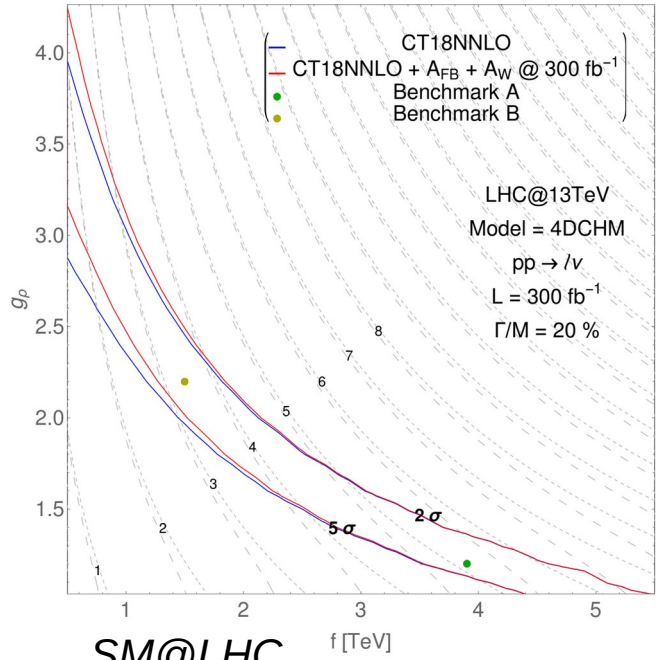

- Depletion of events in the dip region from strong interference effects in the neutral channel can be used to set strong model dependent constrains.
- Predictions for the dip region are sensibly improved by the profiling.
- Searches in the charged channel are more constraining.
- In the charged channel smaller improvement from PDF profiling in the dip region because of milder interference effects.
- Combined searches can improve the limits exploiting the correlation between neutral and charged resonances.

BSM searches in the 4DCHM

Peak region

Dip region

Neutral channel

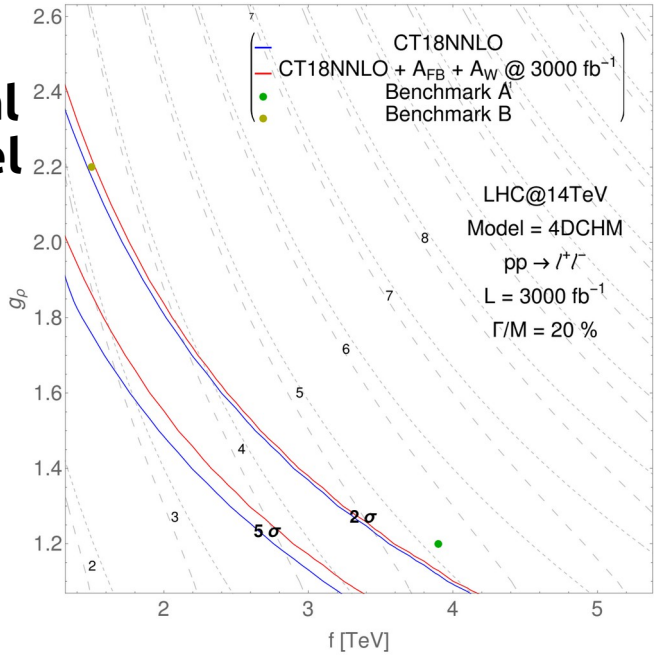

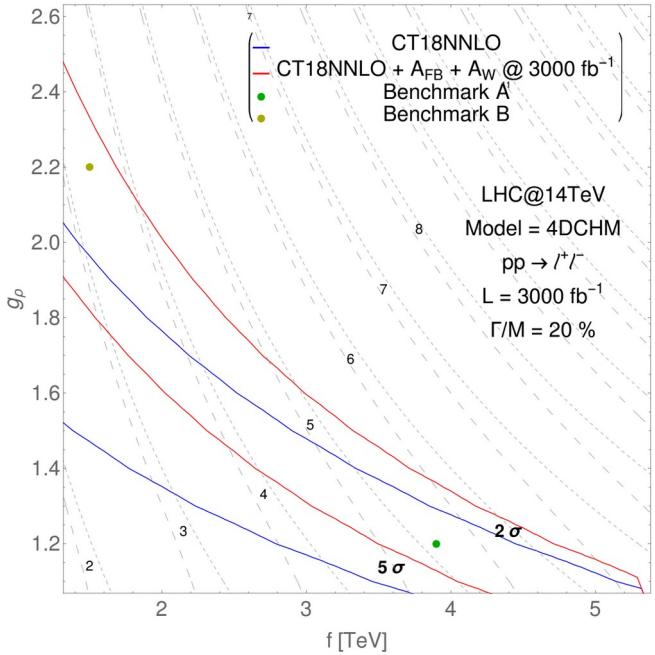

Charged channel

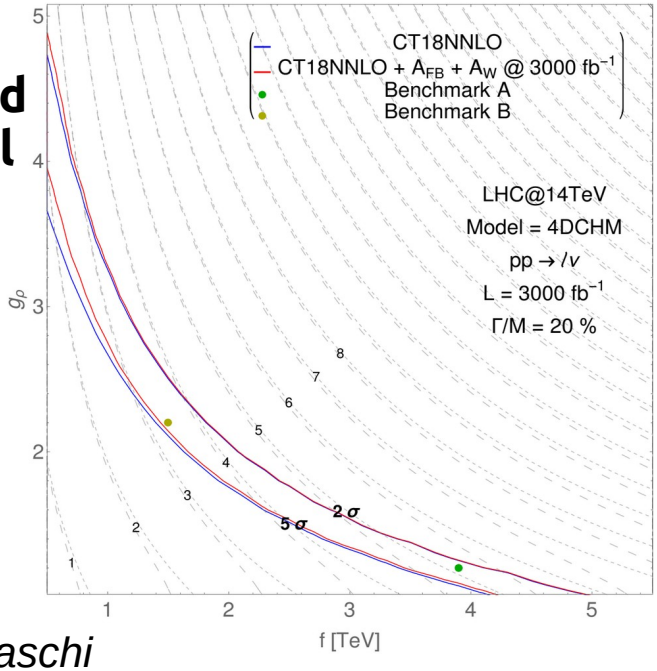

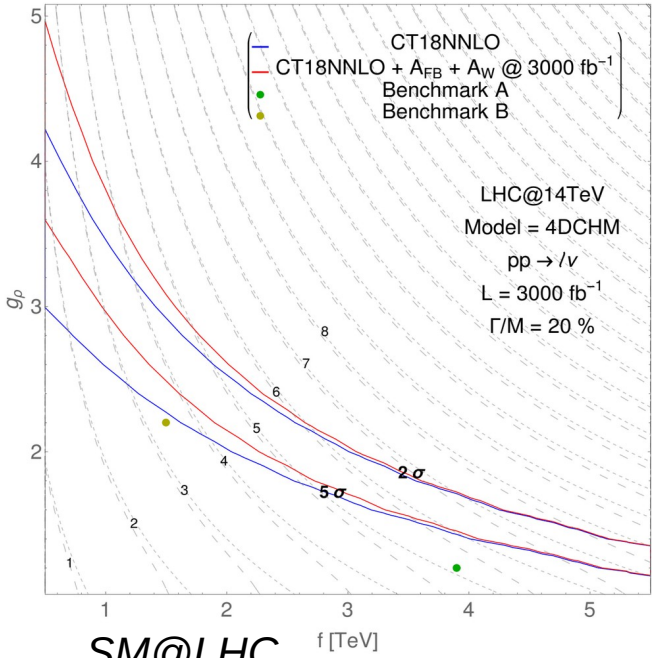

- Depletion of events in the dip region from strong interference effects in the neutral channel can be used to set strong model dependent constrains.
- Predictions for the dip region are sensibly improved by the profiling.
- Searches in the charged channel are more constraining.
- In the charged channel smaller improvement from PDF profiling in the dip region because of milder interference effects.
- Combined searches can improve the limits exploiting the correlation between neutral and charged resonances.

BSM searches in the 4DCHM

Benchmark resonances sensitivities: Neutral channel

Peak

Benchmark A			
inf [TeV]	sup [TeV]	σ_{SM} [fb]	σ_{SM+BSM} [fb]
4.99	8.90	$1.36 \cdot 10^{-4}$	$3.87 \cdot 10^{-4}$
Δ_{PDF} base [fb]	Δ_{PDF} profiled [fb]	α (base)	α (profiled)
$8.1 \cdot 10^{-5}$	$5.6 \cdot 10^{-5}$	1.31	1.35
Benchmark B			
inf [TeV]	sup [TeV]	σ_{SM} [fb]	σ_{SM+BSM} [fb]
3.36	5.52	$5.97 \cdot 10^{-3}$	$8.34 \cdot 10^{-3}$
Δ_{PDF} base [fb]	Δ_{PDF} profiled [fb]	α (base)	α (profiled)
$9.9 \cdot 10^{-4}$	$5.8 \cdot 10^{-4}$	1.88	2.10

Dip

Benchmark A			
inf [TeV]	sup [TeV]	σ_{SM} [fb]	σ_{SM+BSM} [fb]
2.06	4.99	$1.69 \cdot 10^{-1}$	$1.42 \cdot 10^{-1}$
Δ_{PDF} base [fb]	Δ_{PDF} profiled [fb]	α (base)	α (profiled)
$9.5 \cdot 10^{-3}$	$4.6 \cdot 10^{-3}$	3.34	4.82
Benchmark B			
inf [TeV]	sup [TeV]	σ_{SM} [fb]	σ_{SM+BSM} [fb]
1.36	3.36	1.53	1.45
Δ_{PDF} base [fb]	Δ_{PDF} profiled [fb]	α (base)	α (profiled)
$6.8 \cdot 10^{-2}$	$3.1 \cdot 10^{-2}$	1.53	2.91

Benchmark A

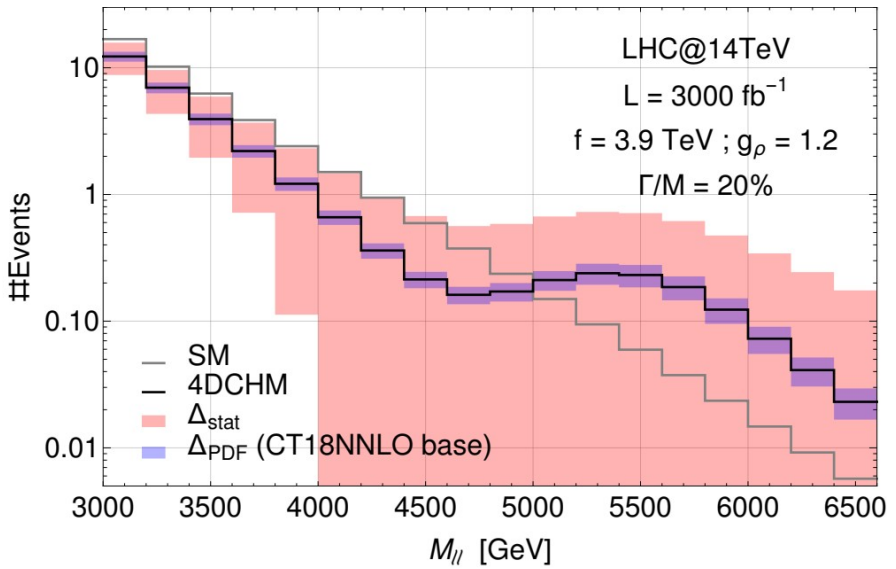

Benchmark B

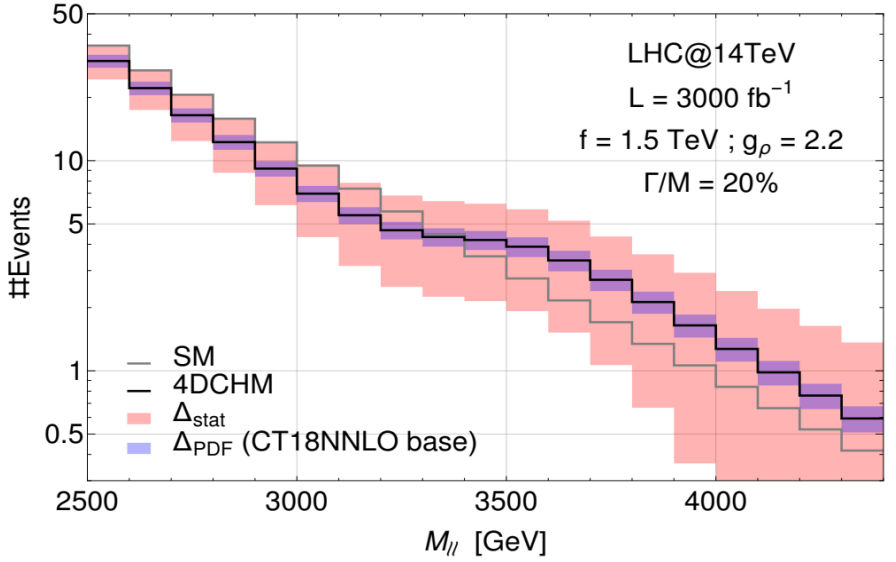

BSM searches in the 4DCHM

Benchmark resonances sensitivities: Charged channel

Peak

Benchmark A			
inf [TeV]	sup [TeV]	σ_{SM} [fb]	σ_{SM+BSM} [fb]
4.11	8.90	$8.13 \cdot 10^{-4}$	$3.51 \cdot 10^{-3}$
Δ_{PDF} base [fb]	Δ_{PDF} profiled [fb]	α (base)	α (profiled)
$6.1 \cdot 10^{-4}$	$5.3 \cdot 10^{-4}$	2.69	2.75
Benchmark B			
inf [TeV]	sup [TeV]	σ_{SM} [fb]	σ_{SM+BSM} [fb]
3.03	5.52	$1.22 \cdot 10^{-2}$	$2.36 \cdot 10^{-2}$
Δ_{PDF} base [fb]	Δ_{PDF} profiled [fb]	α (base)	α (profiled)
$2.3 \cdot 10^{-3}$	$1.9 \cdot 10^{-3}$	4.00	4.24

Dip

Benchmark A			
inf [TeV]	sup [TeV]	σ_{SM} [fb]	σ_{SM+BSM} [fb]
2.22	4.11	$1.07 \cdot 10^{-1}$	$5.71 \cdot 10^{-2}$
Δ_{PDF} base [fb]	Δ_{PDF} profiled [fb]	α (base)	α (profiled)
$3.7 \cdot 10^{-3}$	$2.7 \cdot 10^{-3}$	11.16	12.21
Benchmark B			
inf [TeV]	sup [TeV]	σ_{SM} [fb]	σ_{SM+BSM} [fb]
1.38	3.03	1.60	1.36
Δ_{PDF} base [fb]	Δ_{PDF} profiled [fb]	α (base)	α (profiled)
$5.7 \cdot 10^{-2}$	$3.6 \cdot 10^{-2}$	5.51	7.89

Benchmark A

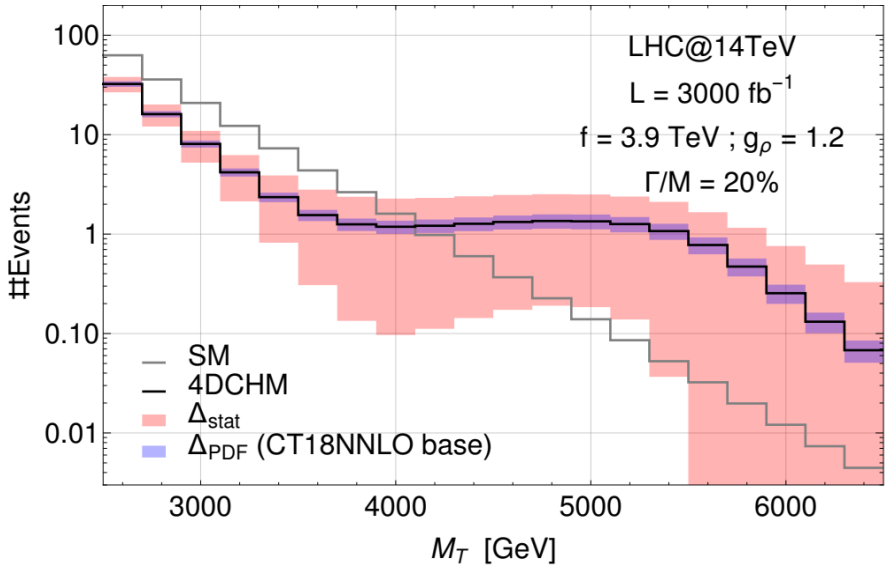

Benchmark B

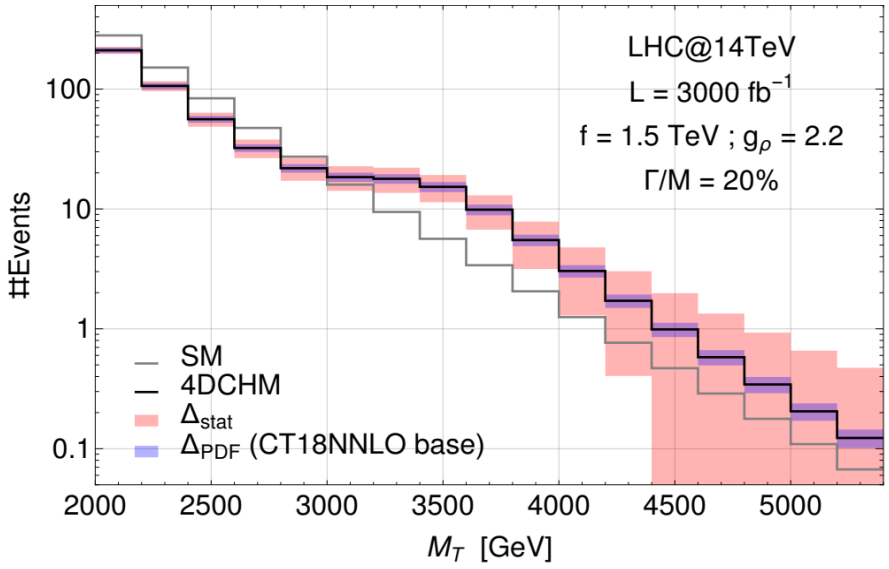

Benchmark analysis

Benchmark	f [TeV]	g_ρ	M_{Z_2} [TeV]	M_{Z_3} [TeV]	M_{W_2} [TeV]	M_{W_3} [TeV]
A	3.9	1.2	5.16	5.56	5.56	6.62
B	1.5	2.2	3.39	3.45	3.45	4.67

Neutral channel

Peak

Benchmark A			
inf [TeV]	sup [TeV]	σ_{SM} [fb]	σ_{SM+BSM} [fb]
4.99	8.90	$1.36 \cdot 10^{-4}$	$3.87 \cdot 10^{-4}$
Δ_{PDF} base [fb]	Δ_{PDF} profiled [fb]	α (base)	α (profiled)
$8.1 \cdot 10^{-5}$	$5.6 \cdot 10^{-5}$	1.31	1.35

Benchmark B			
inf [TeV]	sup [TeV]	σ_{SM} [fb]	σ_{SM+BSM} [fb]
3.36	5.52	$5.97 \cdot 10^{-3}$	$8.34 \cdot 10^{-3}$
Δ_{PDF} base [fb]	Δ_{PDF} profiled [fb]	α (base)	α (profiled)
$9.9 \cdot 10^{-4}$	$5.8 \cdot 10^{-4}$	1.88	2.10

Dip

Benchmark A			
inf [TeV]	sup [TeV]	σ_{SM} [fb]	σ_{SM+BSM} [fb]
2.06	4.99	$1.69 \cdot 10^{-1}$	$1.42 \cdot 10^{-1}$
Δ_{PDF} base [fb]	Δ_{PDF} profiled [fb]	α (base)	α (profiled)
$9.5 \cdot 10^{-3}$	$4.6 \cdot 10^{-3}$	3.34	4.82

Benchmark B			
inf [TeV]	sup [TeV]	σ_{SM} [fb]	σ_{SM+BSM} [fb]
1.36	3.36	1.53	1.45
Δ_{PDF} base [fb]	Δ_{PDF} profiled [fb]	α (base)	α (profiled)
$6.8 \cdot 10^{-2}$	$3.1 \cdot 10^{-2}$	1.53	2.91

Charged channel

Benchmark A			
inf [TeV]	sup [TeV]	σ_{SM} [fb]	σ_{SM+BSM} [fb]
4.11	8.90	$8.13 \cdot 10^{-4}$	$3.51 \cdot 10^{-3}$
Δ_{PDF} base [fb]	Δ_{PDF} profiled [fb]	α (base)	α (profiled)
$6.1 \cdot 10^{-4}$	$5.3 \cdot 10^{-4}$	2.69	2.75

Benchmark B			
inf [TeV]	sup [TeV]	σ_{SM} [fb]	σ_{SM+BSM} [fb]
3.03	5.52	$1.22 \cdot 10^{-2}$	$2.36 \cdot 10^{-2}$
Δ_{PDF} base [fb]	Δ_{PDF} profiled [fb]	α (base)	α (profiled)
$2.3 \cdot 10^{-3}$	$1.9 \cdot 10^{-3}$	4.00	4.24

Benchmark A			
inf [TeV]	sup [TeV]	σ_{SM} [fb]	σ_{SM+BSM} [fb]
2.22	4.11	$1.07 \cdot 10^{-1}$	$5.71 \cdot 10^{-2}$
Δ_{PDF} base [fb]	Δ_{PDF} profiled [fb]	α (base)	α (profiled)
$3.7 \cdot 10^{-3}$	$2.7 \cdot 10^{-3}$	11.16	12.21

Benchmark B			
inf [TeV]	sup [TeV]	σ_{SM} [fb]	σ_{SM+BSM} [fb]
1.38	3.03	1.60	1.36
Δ_{PDF} base [fb]	Δ_{PDF} profiled [fb]	α (base)	α (profiled)
$5.7 \cdot 10^{-2}$	$3.6 \cdot 10^{-2}$	5.51	7.89

The angular coeficient A_0

- $\mathbf{A_0}$ coefficient is parity conserving and sensitive to the flavor singlet PDFs.
- Can be contructed from longitudinal and unpolarized cross sections:

$$A_0(s, M, Y, p_T) = \frac{2d\sigma^{(L)}/dM\,dY\,dp_T}{d\sigma/dM\,dY\,dp_T}$$

- It has been calculated at NNLO QCD (good convergence of perturbative expansion).
  JHEP 11 (2017) 003
- NLO EW corrections are small at high p_T^Z.
  EPJC 80 (2020) 10

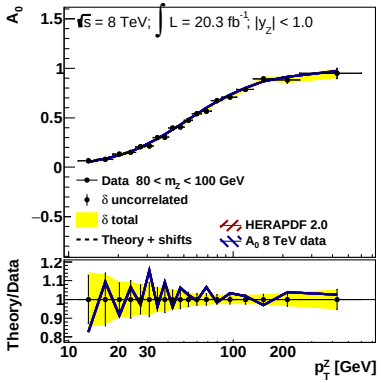

PDF set	Total χ^2/d.o.f.
CT18NNLO	59/53
CT18Annlo	44/53
NNPDF31_nnlo_as_0118_hessian	60/53
ABMP16_5_nnlo	62/53
MSHT20nnlo_as118	59/53
HERAPDF20_NNLO_EIG	60/53

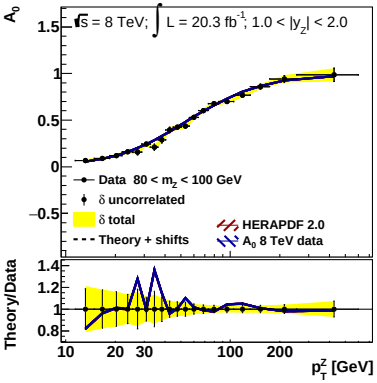

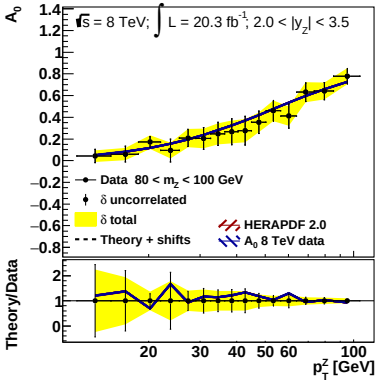

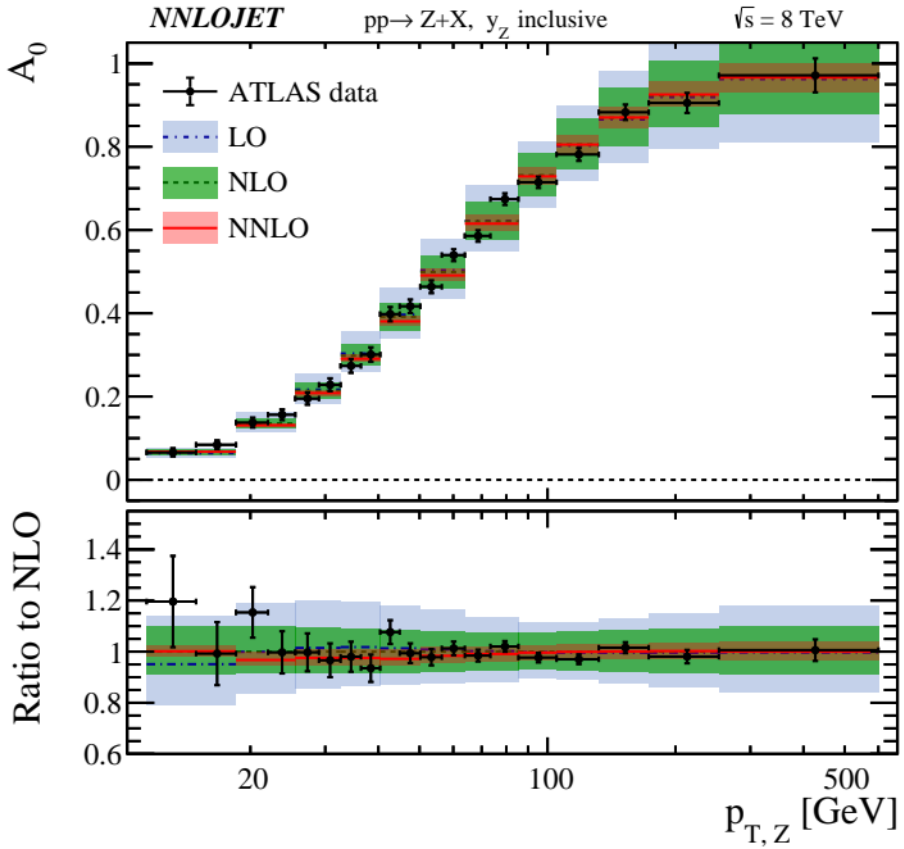

Validation of the implementation of the observable in xFitter:

- 3 rapidity bins
- p_T > 11.4 GeV
- Predictions at order $\boldsymbol{\alpha_s^2}$ from MadGraph5_aMC@NLO
- Covariance matrix of experimental uncertainties included

Good description of the data from modern PDFs

The angular coeficient A_0

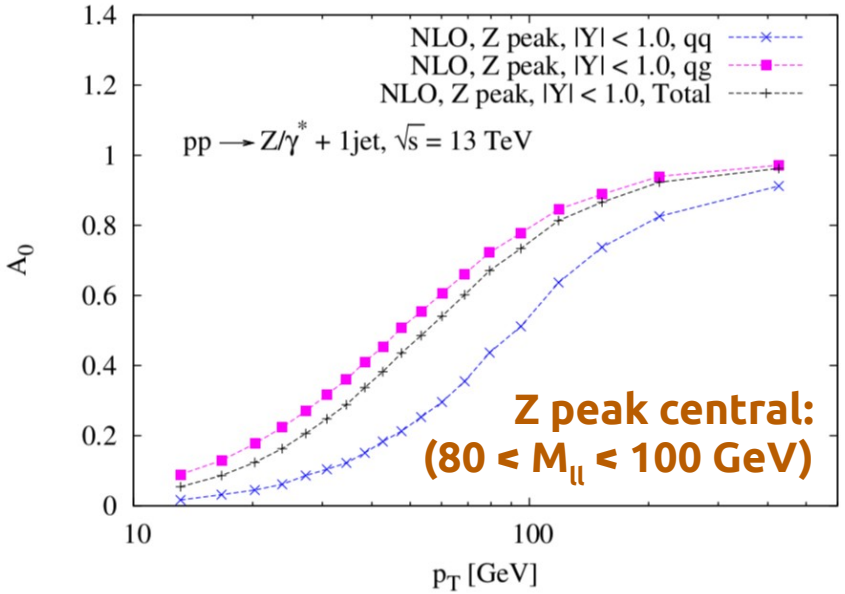

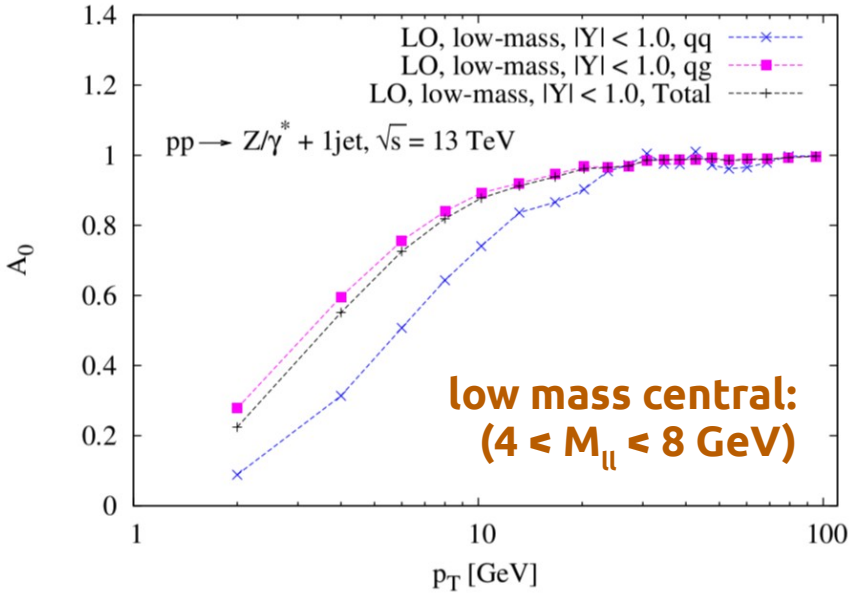

- **A_0** pseudodata evaluated in different invariant mass regions and rapidity ranges.
- Contributions from both $q\bar{q}$ and qg channels.
- Largest sensitivity on PDFs in the region at the saddle point ($\partial^2 A_0 / \partial p_T^2 = 0$).
- Pseudodata generated for 13 TeV c.o.m. energy and projected statistical uncertainties for **300** and **3000 fb^{-1}** luminosity.
- 0.1% systematic uncertainty on leptons momentum scale.

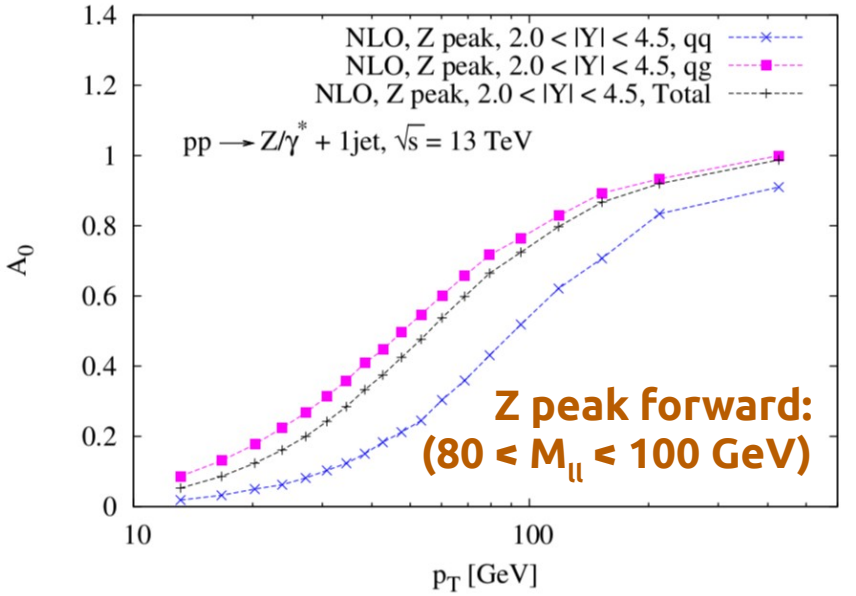

A_0 @ Z peak

- Profiling of xg, xg/Σ, $x\bar{u}$, $x\bar{d}$
- Largest constrains in the region $10^{-3} < x < 10^{-1}$
- Largest impact from 300 fb^{-1} data, but 3000 fb^{-1} data can further constrains $x\bar{u}$, $x\bar{d}$
- Results are stable against variations of ren/fact scales

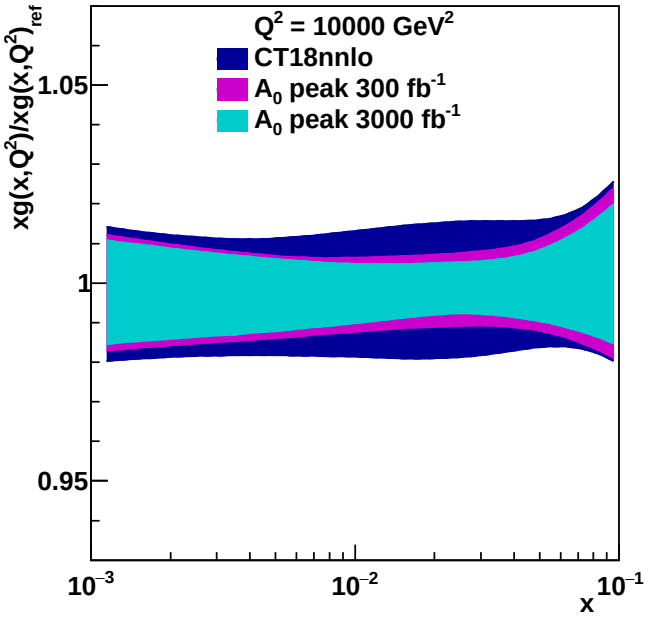

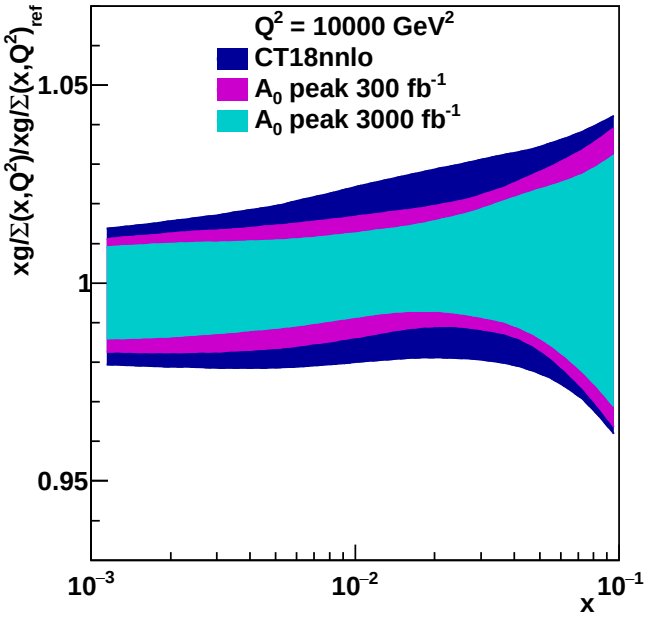

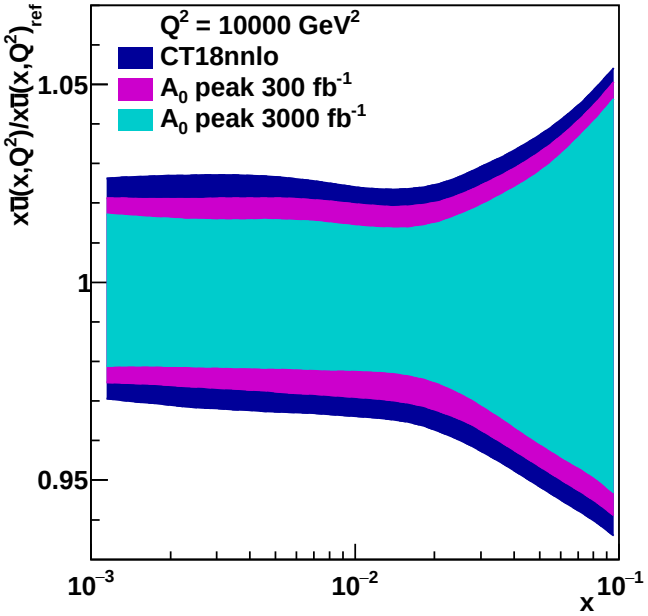

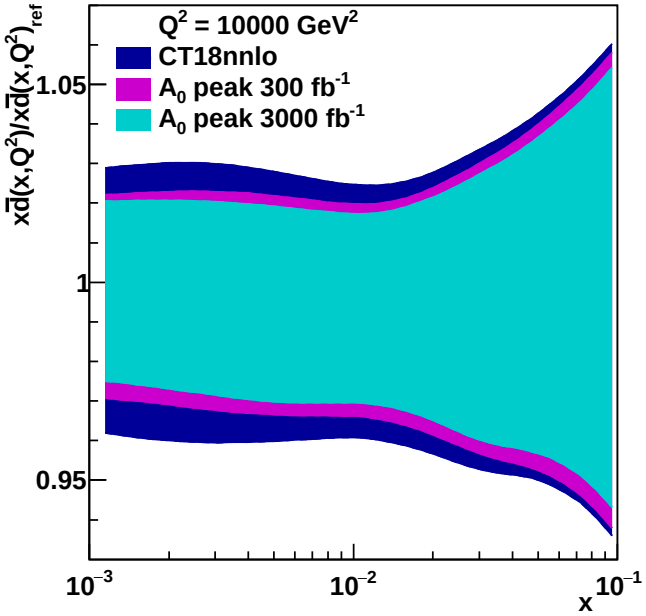

A_0 @ low mass and high rapidity

- Profiling using low invariant mass data

  ($4 < M_{ll} < 8$ GeV)

  - Sensitive to gluon PDF at low-x, $x < 10^{-3}$
  - Possibly useful for TMD PDFs determination

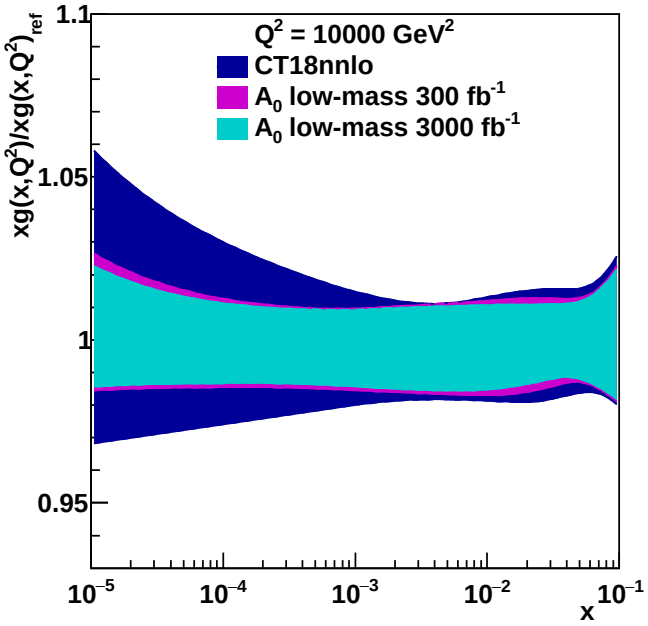

- Profiling using forward rapidity region (LHCb reach):

  ($2.0 < y_{ll} < 4.5$)

  - Improvements in sea quark PDFs at intermediate x, $x \sim 10^{-3}$

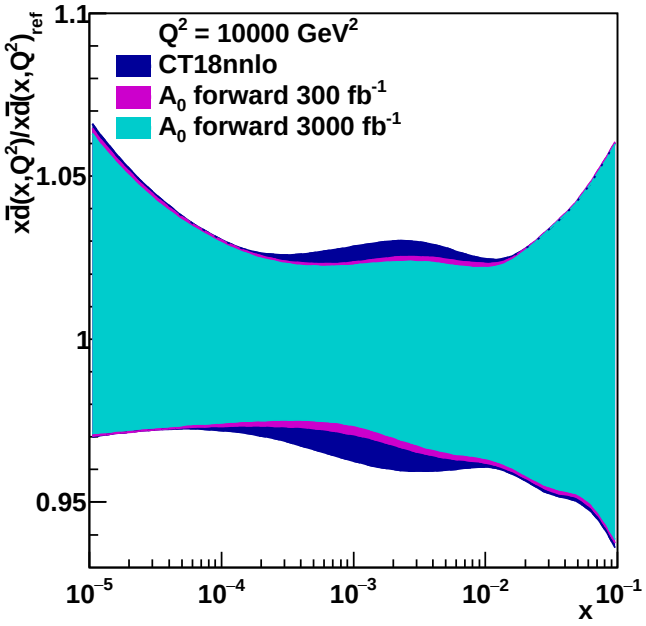

Impact of A_0 on Higgs cross section

- Gluon-gluon luminosity as function of M_X computed at NLO QCD with MCFM.

- PDF uncertainties are reduced by 30%-40% in the Run-III scenario and about 50% in the HL-LHC scenario in the region **$100 < M_X < 200$ GeV** .

- Reduction of uncertainties concentrated in the central rapidity region **$|y_H| < 2.0$** .

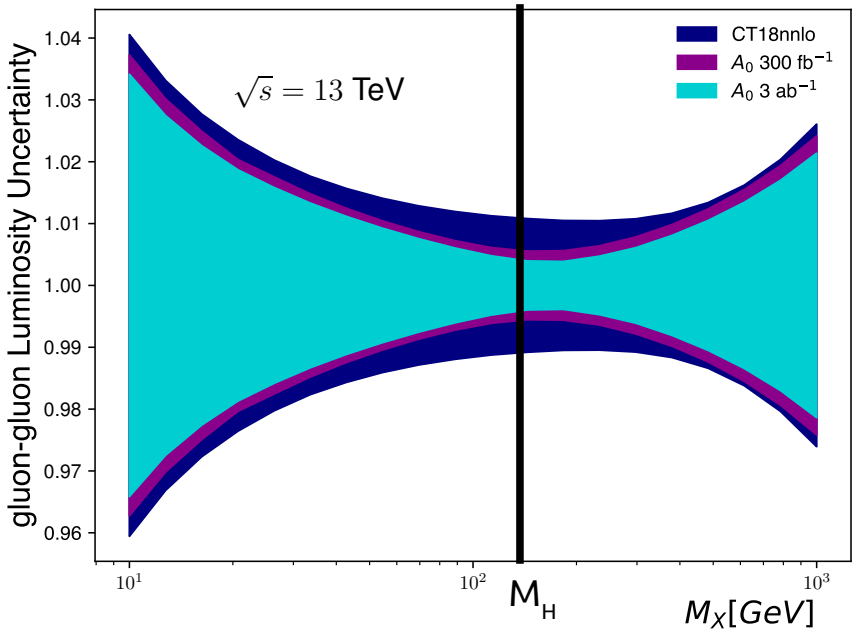

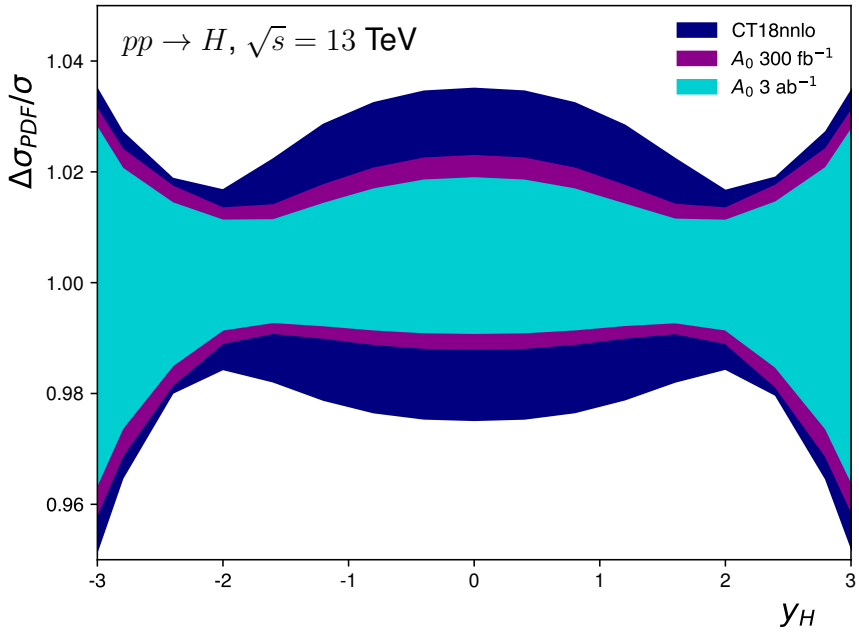

Impact of A_0 on Higgs cross section

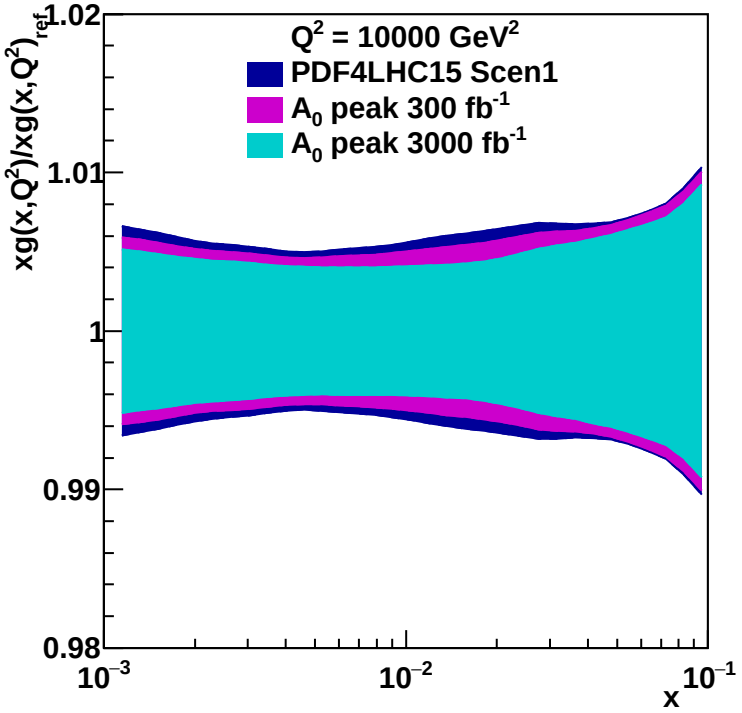

- Profiling projected PDFs based on complete HL-LHC data sample (include jet and top measurements). EPJC 78 (2018) 11
- Further reduction of uncertainty can be obtained.

- In ggF computed at N^{3}LO, the reduction of uncertainty is visible in all modern and projected PDF sets.